

AUTHORS' RESPONSE TO REVIEWERS

We thank the reviewers and Dr. Nassar for their helpful comments that improved the manuscript. The authors' response to the short comment and three reviewers are listed below in order of submission by the reviewers. The reviewers' comments are italicized while responses are in plain text.

SC1 (Ray Nassar):

"Tropospheric column ozone response to ENSO in GEOS-5 assimilation of OMI and MLS ozone data" by Olsen, Wargan and Pawson is a nice study that investigates the impact of ENSO on ozone in both the tropics and midlatitudes, making use of a 9-year GEOS-5 assimilation and a 22-year CTM simulation.

One point that I would like to dispute, however, is the claim in the abstract of "a newly-identified two-lobed response symmetric about the equator in west Pacific/Indonesia region consistent with large scale vertical transport." Section 4.1 mentions that in Oman et al. (2013) the structure was observed by TES, but not in the model and Lines 492- 496, goes on to conclude that this symmetric two-lobed response of ozone in the region is a "novel" finding.

Since they already provide one example of evidence of the two-lobes observed in TES O3, use of the phrase "novel" should be avoided. Two other examples of studies that found these two lobes are Chandra et al. (2009) and Nassar et al. (2009), both of which they have failed to cite anywhere in their manuscript. These studies showed the two-lobe pattern in ozone anomalies by taking the difference of 2006 and 2005 tropospheric ozone. Chandra et al. (2009) used OMI and MLS data along with the GMI model, while Nassar et al. (2009), used TES and GEOS-Chem. In Nassar et al. (2009), we identified that a two-lobe pattern symmetric about the equator, most evident in December anomalies, is primarily of dynamical origin, while fire emissions (via CO oxidation) contributed a single-lobe pattern primarily in October and November (see figure 8). I would suggest updating the manuscript by removing the word "novel" and the phrase "newly-identified" as well as adding a very brief description of the two studies mentioned here.

We thank Dr. Nassar for his short comment related to this manuscript. Although Oman et al. (2013) does not particularly note the two-lobed response in their study, we did overlook the results and discussion made by Dr. Nassar and colleagues in their study. They nicely demonstrate the dynamical origin of the two-lobe response and the chemical origin of the single-lobe response occurring earlier in the year. We greatly appreciate Dr. Nassar for pointing this out and we have modified the manuscript accordingly. The references in the abstract and manuscript to the response as new or novel have been removed. In addition, we have added a comparative discussion of the two-lobe response relative to the Nassar et al. and Chandra et al. studies in our Section 4.1.

RC1 (Referee #3):

...Overall the article is well-written and the topic of the investigation is clearly established. The article makes an important point that although the effects of ENSO on TCO are generally small in midlatitudes, they are imperative to consider when modeling is performed studying TCO anthropogenic vs. natural variability. I think the article could be improved by adding a few references regarding spatial characterization of the ENSO influence on TCO. For the future work it may be interesting to look at different layers of free tropospheric ozone and to investigate how they respond to ENSO. I approve this article for publication with a few minor suggestions.

We thank the reviewer for their helpful suggestions that have improved the manuscript.

Specific Suggestions

On line 41 it states, "This study provides the first explicit spatially resolved characterization. . ." This is a strong statement and probably should be backed up with some kind of reference. The same occurs on lines 509-511.

We have added "near-global" to the qualification since it is an important distinction the spatial characterization in our study is not confined to the tropics and not limited to regional analysis in the extratropics. Other studies that show the spatially resolved response in the tropics and regional impacts at higher latitudes are referenced later in the text. We have also added the phrase, "To the best of our knowledge,..." at the beginning of this statement.

Lines 56-57 need references.

This statement has been moved down in the paragraph so that it directly precedes the citations supporting it.

In lines 66-67, perhaps Thompson et al. 2014 can go to the next paragraph (starting from line 76 and onward) as they actually do not find strong correlation between free tropospheric ozonesonde data and ENSO, while Balashov et al. 2014 do indeed find strong correlation between surface ozone and ENSO.

The Thompson et al. (2014) discussion has been moved to the next paragraph as suggested. We've added the statement that they find the correlation is weak even though they remove the ENSO signal from their ozonesonde time series.

In line 192, what about a trend in ozone? It may be a good idea to detrend TCO monthly mean time series to see purer ENSO signal in the ozone data.

We chose not to detrend the TCO time series since the TCO can respond to the trend in the ENSO signal itself.

Perhaps Figures 1 and 6 could be larger?

The width of these figures was chosen to be close to one column. Although these figures are generally much smaller than the other figures, we feel that using two columns is not needed for the simple line plots compared to the more detailed contour plots, etc.

Lines 251-253 need references.

In response to another reviewer, this sentence has been removed and is not really needed here. The edit does not change the main idea of this subsection.

Technical Comments

In line 420 remove the word "very."

Removed.

RC2 (Referee #4):

...This is a very well written paper with some thorough and convincing analyses presented, and is highly recommended to be published in ACP. There are only some minor points listed below.

Thank you. We've improved the manuscript following the comments addressed below.

Specific comments:

Page 4, lines 107-108: "In the midlatitudes, . . . ENSO in some regions" - Is this the finding from your study (then it should be in your conclusions) or from existing studies, in which case these should be cited?

We find that some readers appreciate having high-level results also presented in the introduction, even though those results may be mentioned in the abstract and conclusion. Thus, readers are reminded and aware of conclusions while going

through the details in the results sections. However, we do see how it may have been confusing whether that statement was referring to our study or previous studies. We modified by explicitly saying that “we show” these results.

Page 5-6, lines 143-146: The description given here is unclear. You write that “some impact from emissions and other tropospheric chemistry sources and sinks is included in the analyses to the extent that each OMI column retrieval is sensitive to tropospheric altitudes”; can you explain what these impact from emissions and other tropospheric chemistry sources and sinks are? Do you mean the OMI column retrieval is sensitive to tropospheric ozone?

We have edited this description to describe that although tropospheric chemistry is not implemented in this version of the assimilation system, increases and decreases to ozone due to chemistry will be included in the analyses through the observations, However, it is limited by the decreasing sensitivity of the OMI retrievals towards the surface.

Page 6, lines 155-157: Although the simulations have been described somewhere else, it would be useful to briefly describe the chemical scheme used in these model simulations, and related boundary conditions (i.e. what sources and sinks are included in the model?).

We added a couple of sentences about the simulated chemistry used in the GMI CTM.

Page 6, line 159: “surface emissions” of what?

We edited to specify the surface emissions as “anthropogenic and biomass burning” emissions.

Page 9, line 249: I wonder why you didn’t mention some significant negative response over the Southern Ocean which are quite obvious.

The Southern Ocean response is now included in the revised manuscript.

Page 13, line 362-364, it would be easier to understand if you express these relationships in a formula, or re-phrase the sentence.

We edited by stating the resulting value would be 5%, which better illustrates the assumed linear, or additive, relationship. It is also then easier to see that $5\%/25\% = 1/5$, which is the value previously stated.

Technical corrections:

Page 10, line 271, delete “in” after “shown”. Page 13, line 366, delete “the” before “both”.

Fixed. Thank you.

RC3 (Referee #1):

...Overall, the results are a nice contribution to the understanding of the connection between ENSO teleconnection and tropospheric ozone variability, although the time period analyzed in the study is quite short (9 years) in a climate standard. The manuscript is within the scope of ACP. However, there are a number of issues in the current manuscript as outlined in my review below. The referee cannot recommend publication of the paper in ACP unless the authors take serious attempt to address these comments in a revised manuscript.

Thank you for your comments. The additional references and discussions suggested have been added to the manuscript as outlined below for each point.

Major comments:

1. Throughout discussions in the manuscript, particularly in the Introduction section reviewing previous work on the extratropical trop. ozone response to ENSO (Lines 56 – 85), the discussions will be more clear if you could add information on the data and time period analyzed in each study. It is known that the different time periods or the number of El Niño or La Niña events included in the analysis often gives very different correlation results given the large internal variability of the mid-latitude atmosphere. For example, Langford et al. (1998, 1999) noted positive correlations between mid-tropospheric and lower-stratospheric ozone observed at Fritz Peak, Colorado during 1994–1998 (without La Niña years), reflecting higher than neutral ozone levels during the El Niño events of 1994–1995 (weak) and 1997–1998 (strong). Lin et al. (2015, Nature Communications) finds that their model captures the observed relationship ($r^2=0.69$) for this short record, but when the entire 1990–2012 period (including both El Niño and La Niña years) is considered, the model indicates little correlation ($r^2=0.18$) between mid-tropospheric and lower-stratospheric ozone over the western US. An extension of the Fritz Peak record to 1999 shows that the mid-tropospheric ozone anomaly in April–May is higher following the La Niña winter of 1998–1999 than in either El Niño or neutral conditions (black circles in Fig. 6c of Lin et al., Nature Communications).

By adding the information on the time period and data used, the readers of the paper could get a sense of how robust the results are.

Throughout the manuscript, the authors tend to contrast their analysis with prior work using shorter records, but not with the recent papers that have examined the

mechanisms controlling the extratropical ozone sensitivity to ENSO events more carefully using longer observations and model simulations.

We have added information about the time periods and data used in the cited studies. We also added additional discussion and comparisons with previous studies that used longer time series. In particular, we compare with the Lin et al. (2014) in Section 3.6, when discussing the reduced variance explained over the Mauna Loa region with our longer 22-year simulation. In Section 4.3, we added discussion comparing with Lin et al. (2015) relative to the ENSO influence over the U.S. This also now includes the Lin et al. comparison to the Langford results as the Referee discusses above.

2. In the introduction, you should also discuss the findings of Lin M. et al. (2014, Nature Geoscience) and Neu J. et al. (2014, Nature Geoscience) and data used in their analysis. For instance, you could say:

*“Using 40 years of ozone observations at Mauna Loa Observatory and a chemistry-climate model, Lin et al. (2014) identified a strong link between El Nino events and lower tropospheric ozone enhancements over the subtropical eastern Pacific in winter and spring. Lin et al. (2014) attribute this to the eastward extension and the equatorward shift of the subtropical jet stream during El Nino, which enhances the long-range transport of Asian pollution. Using mid-tropospheric ozone observations from TES during 2005-2010, Neu et al (2014) found ...
(<http://www.nature.com/ngeo/journal/v7/n5/full/ngeo2138.html>)”*

This additional discussion has been added to the Introduction.

*3. Lines 175-177 and Figures 5, 7, and 8: According to your classification of ENSO events, there are only two El Nino events but five La Nina events. I speculate that this will affect the statistical power of the composite analysis shown in Figures 5-8. Can these events be really characterized as “strong” ENSO events? The boreal fall/winter of 2008/2009 included in your La Nina composite is not even classified as an ENSO event based on the +/- 0.5 threshold used by CPO
(http://www.cpc.ncep.noaa.gov/products/analysis_monitoring/ensostuff/ensoyears.shtml)*

Given the nature of regression, we do not correlate with ENSO “events”, but rather the ENSO sea surface temperature (SST) anomaly time series as a whole. In our comparison of the wind and tendency differences, we compare months with magnitudes of SST anomalies greater than 0.75. As stated in the manuscript, this is nearly equal to 1 standard deviation of the time series. We define these months as having “strong” El Niño or La Niña conditions. We do not require the 5 consecutive months of these conditions the CPC uses to color code their chart on the website referenced by the reviewer. Given the value we use as a threshold is about +/- 1 standard deviation of the time series as a whole, we believe that this classification of strong conditions is valid for our comparison of the differences. However, we do see

where the misunderstanding originated. We erroneously referred to strong “events” in the original manuscript where we defined our threshold in Section 2.3 (while correctly referring to strong conditions elsewhere). Therefore, we have edited and corrected the discussion in Section 2.3. Thank you for bringing it to our attention!

4. Lines 230: It is not clear what you mean by “ground-based data”. Ground-based data of what? UTLS ozone, mid-tropospheric ozone, lower tropospheric ozone, or surface ozone? The sensitivity of ozone to ENSO events can depend strongly on the vertical altitude as demonstrated previously by Lin et al. (2015) using Trinidad Head ozonesonde data and surface ozone observations over the western U.S., which should be also cited here.

We replaced with “ground station, FTIR, and ozonesonde data” and added the Lin et al. reference. Other discussions in the manuscript already note these individual studies and the data each uses.

Related to this comment, I also agree with the other reviewer that it would be very nice if you could illustrate and discuss show the sensitivity varies with the altitudes. These new results will be a very nice addition to the TCO sensitivity discussed in the current manuscript.

We also agree with the other reviewer that it will be nice future work to look at the altitude variation. Wargan et al. (2015) and Ziemke et al. (2014) have validated the analysis TCO and upper tropospheric column relative to vertically integrated sondes and other data. However, the tropospheric profile information has not yet been sufficiently validated compared to observations. Thus, the suggested work is beyond the scope of this manuscript.

5. Lines 190-192 and Lines 203-206: It is not clear whether the ozone data is deseasonalized before correlating with the ENSO index. If not, the extent which the sensitivity reported in Figures 3 and 4 is influenced by by correlations on the seasonal time scale? Please discuss.

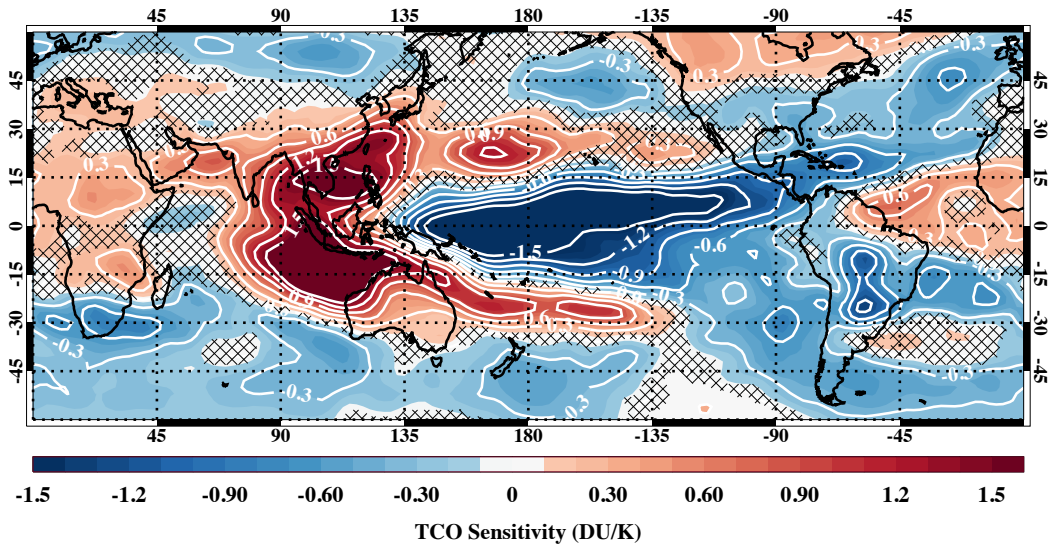
Yes, the ozone data is deseasonalized. In the previous manuscript, the sentence right before Lines 190-192 stated the large season variability was removed by subtracting the respective nine-year mean for each month. We have edited this to explicitly say “deseasonalize”. In Lines 203-206 of the previous manuscript, we already refer to the “deseasonalized TCO”.

6. Lines 251-253: This statement is not true. There are a number of recent studies have extensively examined the mechanisms by which ENSO impacts tropospheric ozone over the extratropical regions, i.e. Lin et al. (2014, 2015) and Neu et al. (2014).

We have removed the statement from the revised manuscript without altering the point of the paragraph.

7. *Figure 10 and associated discussions in the text: It seems like that there is a substantial difference over the subtropical Northeast Pacific. It is surprising that the variance explained by ENSO over the subtropical Northeast Pacific is very weak in the longer record, but analysis of 40 years of observations at Mauna Loa reveals a strong ENSO signature in free tropospheric ozone over this region (Lin et al., 2014, Nature Geosci). Please discuss. Can you also show a comparison similar to Figure 10 but for the sensitivity shown in Figure 4?*

The CTM simulated sensitivity over the same time period is shown below. As is evident, the tropical and extratropical pattern is very similar to that in Figure 4. (The greatest difference is the positive sensitivity found over equatorial Africa and outflow due to biomass burning). We find that the sensitivity over Mauna Loa for the entire simulation is similar. However, the variability of the TCO is up to 20% greater in this region over the longer time period, which can account for some of the difference. We have added discussion relative to this in Section 3.6 (Lines 465-471).



1 **Tropospheric column ozone response to ENSO in GEOS-5**
2 **assimilation of OMI and MLS ozone data**

3

4 **Mark A. Olsen^{1,2}, Krzysztof Wargan^{3,4}, and Steven Pawson³**

5 ¹ Atmospheric Chemistry and Dynamics Laboratory, Code 614, NASA Goddard Space Flight
6 Center, Greenbelt, MD

7 ² Goddard Earth Science, Technology and Research Center, Morgan State University, Baltimore,
8 MD.

9 ³ Global Modeling and Assimilation Office, Code 610.1, NASA Goddard Space Flight Center,
10 Greenbelt, MD

11 ⁴ Science Systems and Applications Inc., Lanham, MD

12 Correspondence to: M. A. Olsen (mark.olsen@nasa.gov)

13

14 **Abstract**

15 We use GEOS-5 analyses of Ozone Monitoring Instrument (OMI) and Microwave Limb Sounder
16 (MLS) ozone observations to investigate the magnitude and spatial distribution of the El Niño
17 Southern Oscillation (ENSO) influence on tropospheric column ozone (TCO) into the middle
18 latitudes. This study provides the first explicit spatially resolved characterization of the ENSO
19 influence and demonstrates coherent patterns and teleconnections impacting the TCO in the
20 extratropics. The response is evaluated and characterized by both the variance explained and
21 sensitivity of TCO to the Niño 3.4 index. The tropospheric response in the tropics agrees well
22 with previous studies and verifies the analyses. [A two-lobed response symmetric about the](#)
23 [Equator in the western Pacific/Indonesian region seen in some prior studies and not in others is](#)
24 [confirmed here. This two-lobed response is](#) consistent with the large-scale vertical transport. We
25 also find that the large-scale transport in the tropics dominates the response compared to the
26 small-scale convective transport. The ozone response is weaker in the middle latitudes, but
27 significant explained variance of the TCO is found over several small regions, including the

Mark Olsen 4/8/2016 11:33 AM

Deleted: However, we show a newly identified

30 central United States. However, the sensitivity of TCO to the Niño 3.4 index is statistically
31 significant over a large area of the middle latitudes. The sensitivity maxima and minima coincide
32 with anomalous anti-cyclonic and cyclonic circulations where the associated vertical transport is
33 consistent with the sign of the sensitivity. Also, ENSO related changes to the mean tropopause
34 height can contribute significantly to the midlatitude response. Comparisons to a 22-year
35 chemical transport model simulation demonstrate that these results from the nine-year
36 assimilation are representative of the longer-term. This investigation brings insight to several
37 seemingly disparate prior studies of the El Niño influence on tropospheric ozone in the middle
38 latitudes.

39

40 1 Introduction

41 The contributions by natural phenomena to tropospheric ozone variability must be identified and
42 quantified for robust assessments of the present and future anthropogenic influence. Here, we
43 investigate the signal of the El Niño Southern Oscillation (ENSO) in extratropical tropospheric
44 ozone in a global assimilation system. To the best of our knowledge, this study provides the first
45 near-global, explicit, spatially resolved characterization of the ENSO influence, and reveals
46 coherent patterns and mechanisms of the influence in the extratropics.

47 ENSO is well known to impact the magnitude of tropospheric ozone in the tropical Pacific. El
48 Niño (La Niña) conditions are characterized by anomalous increases (decreases) in SSTs in the
49 central and eastern Pacific. Opposite anomalies tend to occur in the western Pacific. In general,
50 changes to convection and circulation patterns under El Niño conditions lead to reduced tropical
51 tropospheric ozone in the central and eastern Pacific and enhanced ozone over the western Pacific
52 and Indian Oceans. The response is highly linear in the tropics, so La Niña conditions produce an
53 antisymmetric response (DeWeaver and Nigam, 2002). This influence on tropical tropospheric
54 ozone has been observed in satellite data (e.g., Chandra et al., 1998; Thompson et al., 2001;
55 Ziemke et al., 2010; Ziemke et al., 2015) and ground-based measurements (e.g., Fujiwara et al.,
56 1999; Lee et al., 2010). Both chemical transport models (CTMs) driven by analyzed meteorology
57 and free-running models have simulated this impact of ENSO on the tropical ozone (e.g., Sudo
58 and Takahashi, 2001; Zeng and Pyle, 2005; Doherty et al., 2006; Oman et al., 2011).

Mark Olsen 4/8/2016 5:34 PM

Deleted: T

60 The ENSO impact has also been demonstrated to extend to the subtropics. Using 40 years of
61 ozone observations at Mauna Loa Observatory and a CTM, Lin et al. (2014) identified a strong
62 link between El Niño events and lower tropospheric ozone enhancements over the subtropical
63 eastern Pacific in winter and spring. They attribute this to the eastward extension and the
64 equatorward shift of the subtropical jet stream during El Niño, which enhances the long-range
65 transport of Asian pollution. Neu et al (2014) examined mid-tropospheric ozone
66 observations from TES during 2005-2010 and found increased and decreased zonal mean
67 ozone below the Northern Hemisphere climatological subtropical jet during the 2009-2010
68 El Niño and 2007-2008 La Niña, respectively. ✕

69 In the extratropics, ENSO events have been shown to alter the circulation by modifying planetary
70 wave driving, the North Pacific low, and the location and strength of the extratropical jets (e.g.,
71 Angell and Korshover, 1984; Langford, 1999; Trenberth et al., 2002; García-Herrera et al., 2006).
72 Thus, it is reasonable to expect ENSO to have a dynamical impact on extratropical tropospheric
73 ozone distribution and variability. However, the extratropical ozone response to ENSO has not
74 been as extensively studied as the tropical ozone response and some results from prior studies
75 appear to be contradictory. Oman et al. (2013) examined the ozone sensitivity to ENSO with
76 Microwave Limb Sounder (MLS) and Tropospheric Emission Spectrometer (TES) observations
77 in addition to a chemical-climate model simulation. Although limited by just over five years of
78 TES data (September 2004 through December 2009), they show statistically significant
79 sensitivity in the lower midlatitude troposphere over two broad meridional bands centered on the
80 Pacific and Indian Oceans. Balashov et al. (2014) find a correlation between ENSO and
81 tropospheric ozone around South Africa using air quality monitoring station data from the early
82 1990s to the 2000s. Langford et al. (1998) and Langford (1999) show ozone enhancements in the
83 free troposphere correlated with El Niño (with a several month lag) in lidar data from Boulder,
84 CO between 1993 and 1998. Langford (1999) attributes this to the secondary circulation
85 associated with an eastward shifted Pacific subtropical jet exit region under El Niño conditions.
86 The transverse circulation of ozone-rich air from the stratosphere across the jet is then transported
87 poleward. Lin et al. (2015) conclude that more frequent springtime stratospheric intrusions
88 following La Niña winters contribute to increased ozone at the surface and free troposphere in the
89 western United States.

Mark Olsen 4/12/2016 12:07 PM

Deleted: -

Mark Olsen 4/12/2016 12:22 PM

Formatted: Font:(Default) +Theme Body

Mark Olsen 4/11/2016 10:58 AM

Moved down [1]: The tropospheric ozone response to ENSO in the extratropics has not been as extensively studied and some results from prior studies appear to be contradictory.

Mark Olsen 4/11/2016 10:52 AM

Deleted: extratropical

Mark Olsen 4/11/2016 10:58 AM

Moved (insertion) [1]

Mark Olsen 4/11/2016 10:58 AM

Deleted: The tropospheric ozone response to ENSO in the extratropics has not been as extensively studied and some results from prior studies appear to be contradictory.

Mark Olsen 4/11/2016 3:59 PM

Deleted: and Thompson et al. (2014)

Mark Olsen 4/11/2016 4:00 PM

Deleted: and ozonesonde

Mark Olsen 4/20/2016 11:22 AM

Deleted: NSO

103 In contrast, other observational and modeling studies have not found a significant relationship
104 between ENSO and extratropical tropospheric ozone, suggesting that any such influence is weak
105 or occurs only on a regional scale. For example, Vigouroux et al. (2015) use a stepwise multiple
106 regression model including an ENSO proxy to examine ground-based Fourier transform infrared
107 (FTIR) measurements from eight subtropical and extratropical stations of the Network for the
108 Detection of Atmospheric Composition Change (NDACC). They did not find a significant
109 ENSO impact on the tropospheric ozone column at any of the eight sites. Hess et al. (2015) also
110 did not find a relation between ENSO and tropospheric ozone over extratropical regions in a four-
111 member ensemble model simulation [spanning 1953 to 2005](#). They suggest that ENSO may
112 occasionally induce ozone anomalies but the correlation is weak. [Thompson et al. \(2014\) remove](#)
113 [the ENSO signal from ozonesonde data near South Africa to investigate middle tropospheric](#)
114 [ozone trends. However, in contrast to the results of Balashov et al. \(2014\) using air quality](#)
115 [station data, they find the correlation of the sonde data with ENSO is weak \(A. Thompson,](#)
116 [personal communication\).](#)

117 Determining the spatial extent of ENSO influence on tropospheric ozone from observations is
118 difficult due to the sparse observation networks of sondes, FTIR, etc. The direct retrieval of
119 tropospheric ozone from satellite observations is limited by coarse vertical resolution in the
120 troposphere for nadir-viewing instruments and pressure broadening in the lower troposphere for
121 limb-type instruments. Nevertheless, sonde and surface data combined with satellite observations
122 have been used to derive a coarse global climatology of tropospheric ozone (Logan, 1999).
123 Tropospheric ozone fields have also been derived from subtracting measured stratospheric
124 column ozone from total column ozone (e.g., Fishman et al., 1990; Ziemke et al., 1998; Fishman
125 et al., 2003; Schoeberl et al., 2007). These residual methods are more robust at lower latitudes
126 and have been used to show a large impact by ENSO on tropospheric ozone in the tropics (e.g.,
127 Chandra et al., 1998; Ziemke et al., 1998; Thompson and Hudson, 1999; Ziemke and Chandra,
128 2003; Fishman et al., 2005).

129 The goal of this paper is to use NASA's Goddard Earth Observing System Version 5 (GEOS-5)
130 analyses of satellite measured ozone to investigate the spatial distribution, magnitude, and
131 attribution of the tropospheric ozone response to ENSO. Assimilation provides the advantages of
132 global, gridded fields constrained by observations. Ziemke et al. (2014) show that the ozone

133 assimilation offers more robust tropospheric ozone fields for science applications in the lower and
134 middle latitudes than residual methods. In the present study, the response in the tropics is
135 evaluated and discussed alongside the midlatitude response. The relatively well-established
136 tropical response is primarily included here for verification of the analyses, although several new
137 findings are discussed. The comprehensive examination of the midlatitudes made possible by the
138 ozone assimilation is novel to this study. In the midlatitudes, we show the tropospheric column
139 ozone (TCO) has a statistically significant response to ENSO in some regions. This response can
140 be explained by changes to circulation, convection, and tropopause height. These results will
141 benefit both process-oriented evaluations of the regional ozone response in simulations and
142 assessments of the anthropogenic impact on tropospheric ozone, including prediction of future
143 tropospheric ozone and trends.

144 The following section discusses the data, assimilation system, and methods used in this study.
145 The results are then presented in Section 3. A comparison of results to a CTM simulation is
146 included to show that the nine-year time period of the EOS Aura observations is largely
147 representative of longer periods. Additional discussion of the results is found in Section 4 before
148 concluding with a brief summary.

149

150 **2 Data, assimilation system, and methods**

151 The ozone analyses used in this study were produced using a version of NASA's GEOS-5 data
152 assimilation system (DAS), ingesting data from the Ozone Monitoring Instrument (OMI) and
153 MLS on the Earth Observing System Aura satellite (EOS Aura), as described in Wargan et al.
154 (2015). A brief description of the ozone data and assimilation system is provided in the following
155 subsection. Subsequent subsections provide information on ancillary data sets used and the linear
156 regression analysis used in this study.

157 **2.1 Ozone data and GEOS-5 Data Assimilation System**

158 The OMI and MLS instruments are both onboard the polar orbiting EOS Aura satellite launched
159 on July 15, 2004. OMI is a nadir-viewing instrument that retrieves near-total column ozone
160 across a 60-scene swath perpendicular to the orbit (Levelt et al., 2006). The footprint, or spatial

Mark Olsen 4/8/2016 1:00 PM

Deleted: is found to have

162 resolution, of the nadir scene is 13 km along the orbital path by 24 km across the track. The
163 cross-track scene width increases with distance from nadir to about 180 km at the end rows. OMI
164 collection 3, version 8.5 retrieval algorithm data are used in the analyses considered here. The
165 MLS instrument scans the atmospheric limb to retrieve the ozone vertical profile from microwave
166 emissions. Version 3.3 data on the 38 layers between 261 hPa and 0.02 hPa were used in the
167 present analyses after screening based upon established guidelines (Livesey et al., 2011).

168 The GEOS-5.7.2 version of the data assimilation system is used to produce the ozone analyses.
169 This is a modified version from the system used in the Modern-Era Retrospective analysis for
170 Research and Applications (MERRA) (Rienecker et al., 2011). For the analyses used here, the
171 system uses a $2.5^{\circ} \times 2.0^{\circ}$ longitude-latitude grid with 72 layers from the surface to 0.01 hPa. The
172 vertical resolution around the tropopause is about 1 km. Alongside the ozone data, a large
173 number of in-situ and space-based observations are included in the GEOS-5 analyses (Wargan et
174 al., 2015). However, OMI and MLS ozone retrievals are the only data that directly modify the
175 analysis ozone in this version of the DAS. Anthropogenic and biomass burning ozone production
176 sources are not explicitly implemented in these analyses. Although tropospheric chemistry is not
177 implemented in the assimilation system, ozone that is produced or lost due to emissions and other
178 tropospheric chemistry sources and sinks is included in the analyses to the extent of the
179 sensitivity of each OMI column retrieval at tropospheric altitudes. In general, the sensitivity
180 decreases with decreasing altitude in the troposphere. Wargan et al. (2015) provides more details
181 on the OMI tropospheric sensitivity and the retrieval “efficiency factors”, or averaging kernels,
182 used in the assimilation.

183 Wargan et al. (2015) and Ziemke et al. (2014) previously evaluated these ozone analyses relative
184 to sondes and other satellite data. Their assessments show that accounting for measurement and
185 model errors in the assimilation greatly increases the precision of the tropospheric ozone over
186 other methods of obtaining gridded TCO fields. Both Wargan et al. (2015) and Ziemke et al.
187 (2014) show that there is greater disagreement of the tropospheric ozone analyses with sondes at
188 high latitudes. For this reason, we restrict our discussion in the present study to the tropics and
189 middle latitudes.

190 2.2 Global Modeling Initiative CTM simulation

Mark Olsen 4/19/2016 3:41 PM

Deleted: However,

Mark Olsen 4/8/2016 3:01 PM

Deleted: some impact

Mark Olsen 4/8/2016 3:02 PM

Deleted: from

Mark Olsen 4/8/2016 3:07 PM

Deleted: at

Mark Olsen 4/8/2016 3:07 PM

Deleted: is sensitive to

Mark Olsen 4/8/2016 3:11 PM

Deleted:

Mark Olsen 4/8/2016 3:05 PM

Deleted: (Wargan et al., 2015)

198 We use a Global Modeling Initiative (GMI) CTM (Strahan et al., 2007; Duncan et al., 2008)
199 simulation to determine if the results from the nine years of ozone analyses are representative of
200 the longer term. Stratospheric and tropospheric chemistry are combined in the GMI CTM with
201 124 species and over 400 chemical reactions. The tropospheric chemistry mechanism is a
202 modified version originally from the GEOS-CHEM CTM (Bey et al., 2001). The simulation is
203 driven using MERRA meteorological fields for 1991-2012 and run at the same resolution as the
204 assimilation system. Observation-based, monthly-varying anthropogenic and biomass burning
205 emissions are used through 2010 with repeated 2010 monthly means for the final two years.
206 Strode et al. (2015) provide more details on this specific simulation, which they refer to as the
207 “standard hindcast simulation” in their study. Ziemke et al. (2014) show that the TCO from a
208 similar GMI simulation compares well with sonde observations. In the present study we define,
209 process, and analyze the CTM TCO fields in the same manner as the assimilation fields.

Mark Olsen 4/8/2016 3:53 PM

Deleted: surface

210 2.3 ENSO index and outgoing longwave radiation data

211 ENSO is characterized in this study by the monthly mean Niño 3.4 index available from the
212 NOAA Climate Prediction Center (<http://www.cpc.ncep.noaa.gov/data/indices/>). The index is
213 based upon the mean tropical sea surface temperature between 5° N – 5° S and 170° W – 120° W.
214 This time series is normalized using 1981-2010 as the base time period. Fig. 1 shows the index
215 time series from 1991-2013, which spans the years of the ozone analyses and GMI simulation. In
216 this study, we define months with “strong” El Niño and La Niña conditions as months with index
217 values greater than 0.75 and less than -0.75, respectively. The Climate Prediction Center uses
218 threshold values of 0.5 and -0.5 to characterize El Niño and La Niña, respectively. The value of
219 ± 0.75 used here to characterize months of “strong” conditions is about one standard deviation
220 (0.78) of the time series spanning the assimilation, 2005-2013. La Niña conditions were
221 dominant during the ozone analyses time period (black line in Fig. 1). Months of strong El Niño
222 conditions occurred in the boreal fall/winter of 2006/2007 and 2009/2010. Months of strong La
223 Niña conditions occurred during the boreal fall/winter of 2005/2006, 2007/2008, 2008/2009,
224 2010/2011, and 2011/2012.

Mark Olsen 4/12/2016 12:27 PM

Deleted: events

Mark Olsen 4/12/2016 12:28 PM

Deleted: s

Mark Olsen 4/12/2016 12:28 PM

Deleted: events

Mark Olsen 4/12/2016 12:34 PM

Deleted: s

Mark Olsen 4/12/2016 12:34 PM

Deleted: S

225 We use outgoing longwave radiation (OLR) data as a proxy for convection to investigate the
226 contribution from changes in convection associated with ENSO. The monthly, 1° x 1° data is

233 provided by the NOAA Earth System Research Laboratory (Lee, 2014). Small values of OLR
234 indicate substantial convection, and vice versa.

235 2.4 Methods

236 For the present study, we use the nine full years (2005-2013) of ozone analyses that have been
237 completed. To calculate the TCO, we define the tropopause at each grid point as the lower of the
238 380 K potential temperature and 3.5 potential vorticity unit ($1 \text{ PVU} = 10^{-6} \text{ m}^2 \text{ K kg}^{-1} \text{ s}^{-1}$) surfaces.
239 The daily TCO fields are smoothed horizontally by averaging each grid point with the eight
240 adjacent neighboring points. Monthly mean TCO is computed from the daily values. We
241 deseasonalize the TCO to remove the large seasonal variability by subtracting the respective nine-
242 year mean for each month at each point.

243 We use multiple linear regression of the TCO monthly mean time series onto the Niño 3.4 index
244 and the first four sine and cosine harmonics to evaluate the response of tropospheric ozone to
245 ENSO. That is, $TCO = \sum_i m_i X_i + \varepsilon$, where the X_i are the index and harmonic time series, m_i
246 are the best fit regression coefficients, and ε is the residual error. The regression is computed at
247 every model grid point. The F-test is used to compute the confidence level of the explained
248 variances (Draper and Smith, 1998). The calculated significance of the ozone sensitivity includes
249 the impact from any autocorrelation in the residual time series (Tiao et al., 1990). We find that
250 tests with time-lagged regressions from one to six months were generally no better than for zero-
251 lag regressions. Therefore, the results presented herein are computed with no lag of the ozone
252 time series. This is further discussed in section 4.

253

254 3 Results

255 In this section, we examine the magnitude, spatial distribution, and mechanisms of the TCO
256 response to ENSO. For reference, the multi-year annual mean TCO is shown in Fig. 2. The non-
257 seasonal variability is indicated by overlaid contours of one standard deviation of the
258 deseasonalized TCO expressed as a percent of the mean TCO. (Ziemke et al. (2014) illustrate the
259 large seasonal variability). The following two subsections present the explained variance and
260 TCO sensitivity to the Niño 3.4 index. Changes to advection and convection contributing to the

Mark Olsen 4/7/2016 10:56 AM

Deleted: T

Mark Olsen 4/8/2016 9:42 AM

Deleted: in the TCO is removed at each point

264 TCO response are examined in subsections 3.3 and 3.4. Subsection 3.5 evaluates the ENSO-
265 associated changes to the tropopause height and the impact on the TCO response. We conclude
266 this section with a comparison to CTM results in subsection 3.6 for the purpose of evaluating
267 how robust the results from nine years of ozone assimilation are compared to the longer term.

268 3.1 Explained variance

269 The percent variance of TCO explained by ENSO is shown in Fig. 3. The ENSO influence is
270 greatest in the tropical Pacific where the variance explained has a maximum of about 55%. This
271 well-known tropical response is associated with increased convection and upwelling in the central
272 and eastern Pacific during El Niño that lofts ozone-poor air into the mid- to upper-troposphere.
273 The anomalous warm ocean current that runs southward along the South American coast during
274 El Niño conditions (e.g., Trenberth, 1997) is evident in the tropospheric ozone response. A
275 northeastward tongue of relatively large magnitude also extends towards and across Central
276 America. An isolated significant maximum is also found between 20° N and 30° N in the
277 subtropical Pacific with explained variance of greater than 20%.

278 In the western Pacific and Indonesian region, ENSO is known to produce an opposite response to
279 the central and eastern Pacific due to increased upward transport during La Niña conditions. Two
280 lobes of significant explained variance of more than 20% are symmetric around the equator in
281 this region. Off the western coast of Australia, the southern lobe has a maximum of about 35%.

282 The impact by ENSO is less in the subtropics and middle latitudes compared to the tropical
283 Pacific. Still, the variance explained by ENSO is greater than 20% and statistically significant in
284 several isolated regions. Of particular note, the variance explained exceeds 25% over South
285 Africa and 20% over the central United States. These areas correspond to locations where
286 previous studies have found an ENSO signature in ground [station, FTIR, and ozonesonde](#) data
287 (Balashov et al., 2014; [Langford et al., 1998](#); [Langford, 1999](#); [Lin et al., 2015](#)). The variance
288 explained also exceeds 20% in a small region south of New Zealand. Other midlatitude areas,
289 such as the northern Pacific and Atlantic, exceed 10% but are not statistically significant due to
290 the length of the time series.

291 3.2 TCO sensitivity

Mark Olsen 4/13/2016 4:34 PM

Deleted: -based

Mark Olsen 4/11/2016 11:23 AM

Deleted: Thompson et al., 2014;

294 The sensitivity of TCO per degree change in the Niño 3.4 index is another measure of the ozone
295 response to ENSO determined by the regression analysis. The spatial distribution of the
296 sensitivity is shown in Fig. 4. Over the time period studied here, we find the response to be linear
297 with respect to the ENSO forcing. The large region of negative sensitivity in the central Pacific
298 corresponding to the maximum in explained variance is a result of the increased lofting of ozone-
299 poor air into the middle and upper troposphere under El Niño conditions. Thus, higher values of
300 the Niño 3.4 index correspond to decreases in the TCO. The opposite sensitivity is found in the
301 equatorial symmetric lobes over Indonesia and the eastern Indian Ocean where the increased
302 lofting (decreased TCO) occurs with La Niña (negative Niño 3.4 values). In the subtropics,
303 positive sensitivity is located between about 20° and 30° to the north and south of the large
304 central Pacific minimum. In addition, relatively strong negative sensitivity exists over South
305 Africa corresponding to the significant variance explained there. In the midlatitudes, a negative
306 albeit weaker response is seen over the United States. Statistically significant negative responses
307 are also found over the northern Pacific and Atlantic Oceans, [and the Southern Ocean](#).

308 3.3 Changes in advection

309 We examine the differences in circulation patterns for strong El Niño and La Niña conditions to
310 investigate the large-scale impact of the extratropical circulation relative to the ozone sensitivity.
311 The streamlines of the difference in the mean winds at 200 hPa for months with Niño 3.4 index of
312 greater than 0.75 and less than -0.75 are overlaid on the ozone sensitivity contours in Fig. 4. In
313 the Northern Hemisphere extratropics, anomalous cyclonic circulations coincide with the regions
314 of negative sensitivity over central Asia, the north Pacific, United States, and the north Atlantic.
315 The north Pacific and United States circulations agree well with ENSO-associated upper-
316 troposphere height anomalies observed by Mo and Livezey (1986) and Trenberth et al. (1998).
317 Similar cyclonic circulations aligned with negative sensitivity in the Southern Hemisphere are
318 seen over the southern Pacific Ocean and over the southern tip of South America. Similarly,
319 anomalous anticyclonic flow is associated with positive sensitivity over much of the midlatitudes.
320 The meridional and vertical cross-section streamlines of the difference between the mean winds
321 between 180° W and 120° W for months with Niño 3.4 index greater and less than 0.75 and -0.75
322 respectively are shown in Fig. 5. The positive and negative sensitivity patterns in this region

Mark Olsen 4/11/2016 2:17 PM

Deleted: The manner by which ENSO impacts the TCO is not well established by previous studies for regions relatively far removed from the tropical Pacific ENSO oscillations of sea surface temperatures.

328 shown in Fig. 4 coincide with the anomalous tropospheric downwelling and upwelling. In the
329 tropics, the anomalous upwelling lofts ozone-poor air into the mid- and upper-troposphere in
330 agreement with previous studies. Northward of about 40° N, the tropospheric upwelling
331 coincides with the cyclonic circulation and negative sensitivity shown in Fig. 4. This is
332 consistent with increased upwelling induced by cyclonic circulation. Similarly, other anomalous
333 cyclonic circulations associated with negative sensitivity over North America, the north Atlantic,
334 and the southern tip of South America also correspond to regions of increased upwelling (not
335 shown). The positive sensitivity between about 15° N and 30° N corresponds with increased
336 downwelling and evidence of increased cross-jet transport from the stratosphere into the
337 troposphere in Fig. 5. Oman et al. (2013) find a similar positive sensitivity in this region and also
338 in the Southern Hemisphere subtropics in a GEOS-5 CCM simulation. In addition, Lin et al.
339 (2014) find that increases in springtime ozone following El Niño at the Mauna Loa Observatory
340 in Hawaii correspond to increased influence by Asian pollution. Here, the relative role of ozone-
341 rich pollution transport cannot be distinguished from the cross-jet transport since emissions are
342 not explicitly implemented in the assimilation. The extension of positive sensitivity contours
343 upstream into the western Pacific to Asia in Fig. 4 is consistent with an influence by Asian
344 emissions. However, El Niño and La Niña tend to peak in the Northern Hemisphere winter
345 months when the emissions are least, which would reduce the potential influence.

346 The qualitative interpretation of the upwelling and downwelling shown in Fig. 5 is supported by
347 comparison with the dynamical ozone tendency output by the assimilation system. Fig. 6 shows
348 the differences of the mean dynamical ozone tendencies averaged between 180° W and 120° W
349 for strong El Niño and La Niña months (the black line). The greatest differences occur in the mid
350 to upper troposphere, so the net ozone tendencies are shown for the region between the
351 tropopause and 350 hPa below the tropopause, which provides a constant mass comparison. In
352 the tropics, the El Niño – La Niña difference in the dynamical tendencies ranges between -0.2 to -
353 0.55 DU day⁻¹, consistent with greater upward transport of ozone-poor air during El Niño than La
354 Niña. In the lower extratropics, the dynamical tendency differences increase to around 0.2 DU
355 day⁻¹, corresponding with positive ENSO sensitivity in these regions and increased ozone during
356 El Niño. Negative values of about -0.1 DU day⁻¹ exist between 40° and 50° latitude that
357 correspond with negative sensitivity and upwelling. The small magnitudes at these latitudes are

Mark Olsen 4/8/2016 5:24 PM

Deleted: in

359 about 1/6 of the maximum tropical magnitude, which is consistent with the ratio of the
360 sensitivities in these regions.

361 The positive sensitivity in the tropics around Indonesia corresponds with increased upwelling
362 during La Niña conditions rather than with El Niño. This is evident in the downward oriented
363 streamlines in Fig. 7 showing the circulation differences averaged between 85° E and 120° E for
364 strong El Niño – La Niña months. In the tropics, the magnitude of the difference is smallest near
365 the equator, resulting in the northern and southern tropical lobe structure of sensitivity maxima
366 seen in Fig. 4. The difference is greater in the Southern Hemisphere and the streamlines indicate
367 more stratosphere to troposphere transport than in the Northern Hemisphere as a possible reason
368 for the greater sensitivity in the southern lobe located around 15° S.

369 **3.4 Changes in convection**

370 In addition to the resolved advective vertical transport and stratosphere to troposphere transport,
371 TCO can also respond to ENSO through changes in the vertical transport due to convection and
372 mean depth of the tropospheric column (the tropopause height). This subsection examines the
373 potential impact from convection using differences in OLR as a proxy. Changes in the
374 tropopause height are presented in the following subsection.

375 The differences in the mean OLR for months with Niño 3.4 indices greater and less than 0.75 and
376 -0.75 over the nine years are shown in Fig. 8. The central Pacific is dominated by decreased OLR
377 by up to 25%, indicating greater convection under El Niño conditions. The maximum decrease is
378 displaced to the west of the extrema of explained variance and TCO sensitivity to ENSO (Fig. 3
379 and 4, respectively). Over the Indonesian region, the OLR is increased by up to 16%, indicating
380 reduced convection. Here, the maximum OLR changes are offset to the east of the explained
381 variance and sensitivity extrema.

382 These spatial offsets suggest that much of the tropical TCO sensitivity to ENSO is realized
383 through the resolved advective transport. This is supported by the comparison of the analyses
384 convective and dynamical tendency differences. Fig. 6 compares the El Niño – La Niña
385 differences in the analysis mid to upper tropospheric convective ozone tendencies (red line) and
386 dynamical tendencies (black line) between 180° W and 120° W. In the tropics, the convective
387 tendency differences range from -0.15 to 0.1 DU day⁻¹. The dynamical tendency differences are

388 negative and the magnitudes are more than twice as great as the convective tendency differences.
389 In the middle latitude north Pacific between 40° N and 50° N, the magnitude of the El Niño – La
390 Niña convective ozone tendency difference is similar to the dynamical tendency differences (Fig.
391 6). Thus, the impact on the TCO sensitivity from the resolved transport and convection in this
392 region are comparable in contrast to the tropics where the resolved transport is dominant.

393 **3.5 Impact from tropopause height differences**

394 The sensitivity of the tropopause pressure to the Niño 3.4 index determined by regression
395 analysis is shown in Fig. 9. The response of the tropopause pressure is generally symmetric
396 about the equator over the Pacific Ocean. Under El Niño conditions, a slightly greater mean
397 tropopause pressure (decreased height and shorter tropospheric column) occurs in the extratropics
398 poleward of the climatological subtropical jet. Equatorward, decreased tropopause pressures
399 occur with El Niño, except in the western tropical Pacific where there is a small positive
400 response. The pattern of tropopause response in the Pacific is similar to the 200 hPa circulation
401 anomalies in Fig. 4. The offset of the tropical response extrema to the north and south of the
402 equatorial TCO response (Fig. 4) indicates that very little of the equatorial TCO response is
403 attributable to changes in the depth of the tropospheric column. The maxima TCO response
404 around 25° N and 25° S generally coincide with where the tropopause height response is zero.
405 This also suggests that the positive TCO response here may be impacted by increased
406 stratosphere to troposphere transport of ozone rich air across the subtropical jet.

407 Changes in the depth of the tropospheric column associated with ENSO have a greater impact on
408 the TCO sensitivity in the middle latitudes than in the tropics. Throughout much of the
409 midlatitudes, positive tropopause pressure sensitivity coincides with negative TCO sensitivity and
410 vice versa. Particularly noteworthy in the extratropical Northern Hemisphere are the positive
411 tropopause pressure sensitivity maxima over the northern Pacific, North America, northern
412 Atlantic, and Asia. The positive and negative tropopause sensitivity over extratropical South
413 America also aligns closely to the TCO response.

414 Both the changes in transport (including vertical advection, convection, and cross-tropopause
415 transport) and the tropopause height can impact the magnitude of TCO. We use regression
416 analysis of the mean tropospheric mixing ratio on the Niño 3.4 index to make a rough estimate of

417 the relative influences of transport and tropopause height changes. The mean mixing ratio is
418 directly sensitive to changes in the transport but not to the tropopause pressure. Note that the
419 mean mixing ratio also inherently includes any dependence from changes in chemistry that are
420 associated with ENSO (Sudo and Takahashi, 2001; Stevenson et al., 2005; Doherty et al., 2006).
421 If the response is assumed linear with respect to changes in transport/chemistry and tropospheric
422 column depth, the variances explained by the TCO and mean mixing ratio can provide a first
423 order estimate of the relative roles of these factors. For example, if the TCO explained variance
424 in a region is 25% and the mixing ratio explained variance is 20%, the tropopause height would
425 account for an estimated 5%, or 1/5, of the TCO response.

426 The spatial pattern of the mean mixing ratio explained variance (not shown) is very similar to the
427 TCO regression (Fig. 3) in both the tropics and midlatitudes. Throughout the tropics, the
428 magnitudes of the variance explained are nearly identical. Thus, changes in transport/chemistry
429 dominate the TCO response in this region. However, at middle latitudes the explained variance
430 of mean mixing ratio is frequently less than that of the TCO, so the tropopause height plays a
431 greater role. For the previously noted Northern Hemisphere negative sensitivity extrema, we
432 estimate the tropopause height accounts for about a 1/4 of the TCO response to ENSO over the
433 United States, 1/2 of the response over the North Pacific, and 2/3 of the North Atlantic
434 sensitivity. The tropopause height is responsible for about 1/5 of the negative sensitivity around
435 midlatitude South America. Also, only about 1/5 or less of the positive TCO response in the
436 subtropical Pacific around the climatological subtropical jets is attributable to changes in the
437 tropopause height.

438 **3.6 Representativeness of the 9-year assimilation time series**

439 We use the 22-year (1991-2012) GMI CTM simulation described in section 2.2 to show that the
440 results from the nine years of assimilation are representative of the longer-term TCO response to
441 ENSO. The percentage of the simulated TCO variance explained by ENSO during 2005-2012 is
442 shown in Fig. 10a for comparison with the assimilated ozone results over nearly the same time
443 period (i.e., Fig. 3). The spatial distribution of the simulated TCO response is very similar. The
444 maximum variance explained occurs in the central Pacific. The northeast and southeast split
445 towards Central and South America is evident, but the southern fork is not as prominent. In the

Mark Olsen 4/8/2016 5:25 PM

Deleted: the

447 area of Indonesia, the simulated explained variance exhibits the same lobe-like structure
448 symmetric about the equator. The maximum over the subtropical Pacific and isolated maxima
449 over the United States and South Africa also agree well with the assimilated ozone results.

450 Likewise, the ozone sensitivity to ENSO in the simulation is very similar to the results from the
451 assimilation (not shown). The sensitivity patterns previously discussed relative to the
452 assimilation are well represented in the simulation although the magnitude of the sensitivity is
453 generally slightly greater in the simulation.

454 Regression analysis of the 22-year time span of the hindcast simulation reveals that much of the
455 TCO response determined from the nine years of assimilation is consistent with the longer-term
456 response (Fig. 10b). Use of the longer time series also increases the area in which the explained
457 variance is statistically different from zero, particularly in the middle latitudes. The shape and
458 magnitude of the tropical explained variance is similar to the results from the shorter time period.
459 Two differences are the reduced magnitude extending into the Northern Hemisphere Atlantic and
460 the slight equatorward shift in the location of the Southern Hemispheric lobe in the Indonesian
461 region. In the southern subtropical Pacific near 25° S, the maximum in variance explained is
462 more prominent. Conversely, the maximum in the northern subtropical Pacific is suppressed over
463 the longer-term. However, there remains an enhancement of greater than 15% explained variance
464 near 135° W between 15° N and 30° N that is consistent with the shift in the exit region of the
465 subtropical jet and the associated secondary circulation (Langford, 1999). Lin et al. (2014) find a
466 strong ENSO signature in free tropospheric ozone from 40 years of observations over Mauna
467 Loa. This is in the region where the variance explained is reduced in our 22-year simulation
468 compared to the shorter assimilated and simulated time series. The simulated ozone sensitivity
469 around Mauna Loa in the longer time series is very similar to the sensitivity found using the
470 shorter time series (not shown). However, the TCO variability is greater over the longer time
471 period, at least partially accounting for the reduced variance explained.

472 In the extratropical northern Pacific, corresponding to the location of negative sensitivity in Fig.
473 4, the explained variance is 10%-15% and statistically significant. The signal over the United
474 States and South Africa persists in the 22-year regression at over 20% explained variance. Over
475 midlatitude Europe and Asia, the spatial pattern of the explained variance differs between the 22-

476 year and 8-year regression results. This may be indicative of the variability and trends of
477 emissions being much more dominant than the ENSO influence in this region.

478

479 4 Discussion

480 4.1 Tropical response

481 The tropical tropospheric ozone response to ENSO has been extensively studied in many previous
482 observational and model investigations. The tropical response in the OMI/MLS ozone analyses
483 agrees well with these prior investigations and verifies the analyses. However, many studies that
484 evaluate the spatial distribution of the response do not show a two-lobe structure in the western
485 Pacific/Indonesian region as seen in the present study (e.g., Ziemke and Chandra, 2003).
486 Nevertheless, our results confirm that the two-lobed response to the 2006 El Niño seen in OMI-
487 MLS TCO residual fields by Chandra et al. (2009) and in TES observations by Nassar et al.
488 (2009) is a robust response evident when considering more than that single event. Furthermore,
489 Nassar et al. (2009) used a tropospheric CTM to show that this structure is predominantly of
490 dynamical origin rather than from biomass burning emissions. The two-lobe structure is also
491 suggested in the ozone sensitivity computed from regression of 5 years of TES data shown by
492 Oman et al. (2013) in their Fig. 5a. We find that the symmetric response is likewise well
493 simulated by the GMI CTM driven by assimilated meteorology (Fig. 10). However, the free-
494 running GEOS-5 Chemistry Climate Model simulation examined by Oman et al. (2013) produces
495 a single, broad response centered on the Equator (their Fig. 5b) where the vertical wind
496 differences are consistent with the single, centered response. This demonstrates that the ozone
497 response is sensitive to changes in the advective transport that must be well simulated to
498 reproduce the observed tropospheric response.

499 4.2 Timing of the response

500 As discussed in section 2, sensitivity tests of possible lags in the ozone response in the regression
501 analysis did not increase the correlation between the regressed ozone and Niño 3.4 index or
502 increase the explained variance. In general, the correlation and explained variance remain nearly
503 constant or decreasing with lag times of one or two months in the middle latitudes. The

Mark Olsen 4/8/2016 11:39 AM

Deleted: most

Mark Olsen 4/8/2016 11:56 AM

Deleted: We note that

Mark Olsen 4/8/2016 11:40 AM

Deleted: t

Mark Olsen 4/8/2016 11:40 AM

Deleted: is

Mark Olsen 4/8/2016 12:04 PM

Deleted: Tropospheric Emission Spectrometer (TES)

Mark Olsen 4/8/2016 12:34 PM

Deleted:

Mark Olsen 4/8/2016 12:05 PM

Deleted: The

Mark Olsen 4/8/2016 12:34 PM

Deleted: in this region

Mark Olsen 4/11/2016 2:18 PM

Deleted: very

Mark Olsen 4/8/2016 12:34 PM

Deleted:

515 correlations generally decrease rapidly with longer lag times. This lack of improved regressions
516 using longer lag times indicates that there is minimal impact from long-range transport, including
517 transport in the stratosphere that modulates lower stratospheric ozone concentrations and hence,
518 the magnitude of large-scale stratosphere to troposphere exchange of ozone. This is consistent
519 with previous studies that find little relation between ENSO and large-scale stratosphere-
520 troposphere exchange at midlatitudes (e.g., Hsu and Prather, 2009; Hess et al., 2015). In the
521 present study, the changes to transport and tropopause height contributing to the TCO response
522 act over shorter time scales and potentially impact the entire or large portions of the tropospheric
523 column.

524 **4.3 Regional aspects of the midlatitude response**

525 In the middle latitudes, the statistically significant variance explained by ENSO shown in this
526 study occurs over small-scale regions, so it is not surprising that some previous studies fail to find
527 an ENSO influence over large-scale regions or in many surface-based observations. For example,
528 there is no statistically significant explained variance over the midlatitude regions of Canada,
529 Central Europe, and Japan considered by Hess et al. (2015). These regions also remain
530 insignificant in the 22-year CTM simulation in the present study.

531 Conversely, Langford et al. (1998) demonstrate a correlation of ENSO with lidar observations of
532 ozone near Boulder, Colorado [from 1993 to 1998](#). This coincides with the location of significant
533 explained variance and negative sensitivity we show in Figs. 3 and 4. However, Langford et al.
534 (1998) show a positive correlation of mid-tropospheric ozone with the ENSO time series where
535 the ozone signal lags ENSO by a few months. The lidar ozone anomalies are correlated with the
536 subtropical jet exit region in the northeastern Pacific (Langford, 1999). He hypothesizes that
537 transverse circulation across [an El Niño-shifted jet exit region](#) brings stratospheric air into
538 subtropical tropical troposphere where it descends with the secondary circulation and is then
539 transported northward to the central United States. In the present study, the suggestion of
540 increased localized stratosphere-to-troposphere transport and subsequent downwelling in the
541 northern subtropical Pacific is supported by the meridional cross-section of the anomalous wind
542 field (Fig. 5) and the relatively large TCO response evident in the explained variance and
543 sensitivity (Figs. 3 and 4). It is possible that episodic events may bring anomalously high ozone

Mark Olsen 4/12/2016 11:23 AM

Deleted: the ENSO

545 air to the central United States from the subtropics that can impact at least a portion of the
546 tropospheric column. However, we find that the immediate negative influence by the ENSO-
547 driven vertical transport and tropopause height changes is dominant when considering the entire
548 tropospheric column.

549 Furthermore, the model evaluation by Lin et al. (2015) reproduces the positive correlation over
550 the Colorado region for the time period studied by Langford et al. (1998), but the correlation is
551 not evident when they consider the longer time period from 1990 to 2012. They show that more
552 frequent springtime stratospheric intrusions following La Niña winters contribute to increased
553 ozone at the surface and free troposphere in the western United States. Since the stratospheric
554 intrusions are associated with enhanced stratosphere to troposphere transport, this can
555 significantly increase the TCO through an influx of ozone-rich air at lower altitudes. The
556 negative sensitivity over the United States shown in the present study is consistent with these
557 results of Lin et al. (2015).

558 4.4 South African region

559 We find significant explained variance and sensitivity of TCO around subtropical South Africa.
560 This is consistent with the findings of Balashov et al. (2014) who show a correlation of surface
561 observations of ozone with ENSO. They attribute this association to increased ozone formation
562 from anthropogenic emissions under warmer and drier conditions occurring with El Niño.
563 Unlike most of the midlatitude TCO response, the processes that drive the TCO response in the
564 southern Africa region are not clear considering the mechanisms investigated in this study. A
565 meridional cross-section of the difference in the resolved advective winds averaged between 15°
566 E and 55° E for strong El Niño and La Niña months (not shown) does not indicate coherent
567 upwelling consistent with the negative sensitivity found there. Overall, there is weak anomalous
568 downward transport between about 5 km and 11 km in this region. The differences in OLR (Fig.
569 8) are also not consistent with unresolved convection as the source of the negative sensitivity.
570 The tropopause height sensitivity to ENSO in this region (Fig. 9) is positive and similar to the
571 spatial pattern of TCO sensitivity (Fig. 4) but is weak compared to the relatively strong TCO
572 response. Therefore, much of the TCO response may be due to ENSO-related changes in the

Mark Olsen 4/12/2016 11:36 AM
Deleted: .

Mark Olsen 4/12/2016 11:38 AM
Moved down [2]: The negative sensitivity over the United States is consistent with the results of Lin et al. (2015).

Mark Olsen 4/12/2016 11:37 AM
Deleted: conclude

Mark Olsen 4/12/2016 11:38 AM
Moved (insertion) [2]

Mark Olsen 4/12/2016 11:18 AM
Deleted:

Mark Olsen 4/11/2016 11:17 AM
Deleted: previous

Mark Olsen 4/11/2016 11:17 AM
Deleted: .

Mark Olsen 4/11/2016 11:21 AM
Deleted: laI

Mark Olsen 4/11/2016 3:55 PM
Deleted: Thompson et al. (2014) remove the ENSO signal from southern Africa region ozonesonde data to investigate middle tropospheric ozone trends.

586 ozone chemistry, [similar to the Balashov et al. \(2014\) results using surface ozone data](#), although
587 [this](#) requires further investigation beyond the scope of this study.

588

589 5 Summary

590 The assimilation of OMI and MLS data enables this first comprehensive study of the TCO
591 response along with the ancillary information to interpret and explain the results. We have used
592 regression analysis of the TCO to provide an observationally-constrained evaluation of the
593 magnitude and spatial distribution of the ENSO impact on TCO throughout the middle latitudes.
594 Prior results of the TCO response outside the tropics have been contradictory and limited by the
595 spatial distribution and sparseness of available data. The present study is able to unify and explain
596 many aspects of the seemingly disparate findings reported by previous studies.

597 While the examination of the response in the tropics is included primarily for completeness and
598 verification of the analyses, [we particularly note](#) two results. We find that changes in the large-
599 scale transport dominate the changes in convective transport to produce the TCO response
600 throughout much of the tropics. We also show [that](#) a two-lobe response around Indonesia
601 [symmetric about the Equator, seen in prior studies of the 2006 El Niño, is not unique to that](#)
602 [event](#).

603 The midlatitude ozone response to ENSO is not as strong as in the tropics. However, the
604 explained variance is statistically significant over several small regions for the 9-year analysis,
605 such as over the United States and south of New Zealand. Other areas have an explained
606 variance of greater than 10% that the 22-year CTM simulation suggests would be statistically
607 significant with a longer observation period. These regions include the northern Pacific and
608 around midlatitude South America.

609 The TCO sensitivity to ENSO is relatively small but statistically significant over much of the
610 midlatitudes. These regions of negative (positive) sensitivity are coincident with anomalous
611 cyclonic (anticyclonic) circulation. The anomalous circulations are associated with upwelling
612 and downwelling that are consistent with the sign of sensitivity. In addition to the contribution
613 by transport, changes in the tropopause height can contribute substantially to the middle latitude
614 TCO response by altering the depth of the tropospheric column.

Mark Olsen 4/11/2016 11:20 AM

Deleted: that

Mark Olsen 4/8/2016 12:40 PM

Deleted: in this region are novel to this study

Mark Olsen 4/20/2016 2:40 PM

Deleted: in the region

Mark Olsen 4/20/2016 2:40 PM

Deleted: that

Mark Olsen 4/8/2016 12:41 PM

Deleted: is

Mark Olsen 4/8/2016 12:42 PM

Deleted: symmetric about the Equator with maxima near 15° N and 15° S.

623 This study using analyses of OMI and MLS ozone provides the first explicit spatially resolved
624 characterization of the ENSO influence and demonstrates coherent patterns and teleconnections
625 impacting the TCO in the extratropics. Although relatively weak, the ENSO-driven variability
626 needs to be considered in investigations of midlatitude tropospheric ozone, particularly on
627 regional scales. The spatial variability of the TCO response indicates the ENSO influence is
628 likely statistically insignificant for hemispheric studies or over other broad areas. However, the
629 variance explained by ENSO can be 10% or greater over smaller regions like the United States,
630 midlatitude South America, and South Africa. Thus, it will be important in attributing the
631 sources of variability and trends in TCO, such as by human-related activity. These results are
632 potentially useful for evaluating the spatially dependent model response of TCO to ENSO
633 forcing. In the extratropics, the ENSO signal is convolved with large extratropical circulation
634 variability from other sources. Thus, additional factors may need to be considered when
635 evaluating the midlatitude response in free-running models, particularly in ensemble simulations.

636

637 **Acknowledgements**

638 The authors would like to thank Paul Newman, Jerry Ziemke, Luke Oman, Anne Douglass, and
639 Susan Strahan for helpful discussions. In addition, the authors thank Ray Nassar and three
640 anonymous reviewers for their helpful comments that improved the manuscript. Funding for this
641 research was provided by NASA's Modeling, Analysis and Prediction Program and by NASA
642 NNH12ZDA001N-ACMAP. The assimilated data used in this study are available through the
643 Aura Validation Data Center website: <http://avdc.gsfc.nasa.gov>. Simulations and assimilation
644 were done at NASA's Climate Computing Service under awards from HPC. The Niño 3.4 index
645 used in this study is available from the NOAA Climate Prediction Center at
646 <http://www.cpc.ncep.noaa.gov/data/indices/>. The OLR data is provided by the
647 NOAA/OAR/ESRL PSD, Boulder, Colorado, USA, from their web site at
648 <http://www.esrl.noaa.gov/psd/>.

649 **References**

- 650 Angell, J. K., and J. Korshover: Some long-term relations between equatorial sea-surface
651 temperature, the four centers of action and 700 mb flow, *J. Climate Appl. Meteor.*, 23,
652 1326-1332, doi:10.1175/1520-0450(1984)023<1326:SLTRBE>2.0.CO;2, 1984.
- 653 Balashov, N. V., A. M. Thompson, S. J. Piketh, and K. E. Langerman: Surface ozone variability
654 and trends over the South African Highveld from 1990 to 2007, *J. Geophys. Res. Atmos.*,
655 119, 4323-4342, doi:10.1002/2013JD020555, 2014.
- 656 [Bey, I., D. J. Jacob, R. M. Yantosca, J. A. Logan, B. D. Field, A. M. Fiore, Q. Li, H. Y. Liu, L. J.
657 Mickley, and M. G. Schultz: Global modeling of tropospheric chemistry with assimilated
658 meteorology: Model description and evaluation, *J. Geophys. Res.*, 106, 23073-23095,
659 doi:10.1029/2001JD000807, 2001.](#)
- 660 Chandra, S., J. R. Ziemke, W. Min, and W. G. Read: Effects of 1997-1998 El Niño on
661 tropospheric ozone and water vapor, *Geophys. Res. Lett.*, 25, 3867-3870,
662 doi:10.1029/98GL02695, 1998.
- 663 [Chandra, S., J. R. Ziemke, B. N. Duncan, T. L. Diehl, N. J. Livesey, and L. Froidevaux: Effects
664 of the 2006 El Niño on tropospheric ozone and carbon monoxide: implications for dynamics
665 and biomass burning, *Atmos. Chem. Phys.*, 9, 4239-4249, doi:10.5194/acp-9-4239-2009,
666 2009.](#)
- 667 DeWeaver, E., and S. Nigam: Linearity in ENSO's atmospheric response, *J. Climate*, 15, 2446-
668 2461, doi:10.1175/1520-0442(2002)015<2446:LIESAR>2.0.CO;2, 2002.
- 669 Doherty, R. M., D. S. Stevenson, C. E. Johnson, W. J. Collins, and M. G. Sanderson:
670 Tropospheric ozone and El Niño–Southern Oscillation: Influence of atmospheric dynamics,
671 biomass burning emissions, and future climate change, *J. Geophys. Res.*, 111,
672 10.1029/2005JD006849, 2006.
- 673 Draper, N. R., and H. Smith (1998), *Applied Regression Analysis*, John Wiley & Sons, Inc.,
674 Hoboken, NJ, USA.
- 675 Duncan, B. N., J. J. West, Y. Yoshida, A. M. Fiore, and J. R. Ziemke: The influence of European
676 pollution on ozone in the Near East and northern Africa, *Atmos. Chem. Phys.*, 8, 2267-

677 2283, doi:10.5194/acp-8-2267-2008, 2008.

678 Fishman, J., C. E. Watson, J. C. Larsen, and J. A. Logan: Distribution of tropospheric ozone
679 determined from satellite data, *J. Geophys. Res.*, 95, 3599, doi:10.1029/JD095iD04p03599,
680 1990.

681 Fishman, J., A. E. Wozniak, and J. K. Creilson: Global distribution of tropospheric ozone from
682 satellite measurements using the empirically corrected tropospheric ozone residual
683 technique: Identification of the regional aspects of air pollution, *Atmos. Chem. Phys.*, 3,
684 893-907, doi:10.5194/acp-3-893-2003, 2003.

685 Fishman, J., J. K. Creilson, A. E. Wozniak, and P. J. Crutzen: Interannual variability of
686 stratospheric and tropospheric ozone determined from satellite measurements, *J. Geophys.*
687 *Res.*, 110, 10.1029/2005JD005868, 2005.

688 Fujiwara, M., K. Kita, S. Kawakami, T. Ogawa, N. Komala, S. Saraspriya, and A. Surlipto:
689 Tropospheric ozone enhancements during the Indonesian Forest Fire Events in 1994 and in
690 1997 as revealed by ground-based observations, *Geophys. Res. Lett.*, 26, 2417-2420,
691 doi:10.1029/1999GL900117, 1999.

692 García-Herrera, R., N. Calvo, R. R. Garcia, and M. A. Giorgetta: Propagation of ENSO
693 temperature signals into the middle atmosphere: A comparison of two general circulation
694 models and ERA-40 reanalysis data, *J. Geophys. Res.*, 111, 10.1029/2005JD006061, 2006.

695 Hess, P., D. Kinnison, and Q. Tang: Ensemble simulations of the role of the stratosphere in the
696 attribution of northern extratropical tropospheric ozone variability, *Atmos. Chem. Phys.*, 15,
697 2341-2365, doi:10.5194/acp-15-2341-2015, 2015.

698 Hsu, J., and M. J. Prather: Stratospheric variability and tropospheric ozone, *J. Geophys. Res.*,
699 114, 10.1029/2008JD010942, 2009.

700 Langford, A. O.: Stratosphere troposphere exchange at the subtropical jet: Contribution to the
701 tropospheric ozone budget at midlatitudes, *Geophys. Res. Lett.*, 26, 2449-2452,
702 doi:10.1029/1999GL900556/pdf, 1999.

703 Langford, A. O., T. J. O'Leary, C. D. Masters, K. C. Aikin, and M. H. Proffitt: Modulation of
704 middle and upper tropospheric ozone at northern midlatitudes by the El Niño/Southern

705 Oscillation, *Geophys. Res. Lett.*, 25, 2667-26701998.

706 Lee, H.-T., 2014: Climate Algorithm Theoretical Basis Document (C-ATBD): Outgoing
707 Longwave Radiation (OLR) - Daily. NOAA's Climate Data Record (CDR) Program,
708 CDRP-ATBD-0526, 46 pp.
709 [http://www1.ncdc.noaa.gov/pub/data/sds/cdr/CDRs/Outgoing%20Longwave%20Radiation](http://www1.ncdc.noaa.gov/pub/data/sds/cdr/CDRs/Outgoing%20Longwave%20Radiation%20-%20Daily/AlgorithmDescription.pdf)
710 [%20-%20Daily/AlgorithmDescription.pdf](http://www1.ncdc.noaa.gov/pub/data/sds/cdr/CDRs/Outgoing%20Longwave%20Radiation%20-%20Daily/AlgorithmDescription.pdf).

711 Lee, S., D. M. Shelow, A. M. Thompson, and S. K. Miller: QBO and ENSO variability in
712 temperature and ozone from SHADOZ, 1998–2005, *J. Geophys. Res.*, 115,
713 doi:10.1029/2009JD013320, 2010.

714 Levelt, P. F., G. H. J. van den Oord, M. R. Dobber, A. Malkki, V. Huib, J. de Vries, P. Stammes,
715 J. O. V. Lundell, and H. Saari: The ozone monitoring instrument, *Geoscience and Remote*
716 *Sensing, IEEE Transactions on*, 44, 1093-1101, doi:10.1109/TGRS.2006.872333, 2006.

717 Lin, M., L. W. Horowitz, S. J. Oltmans, A. M. Fiore, and S. Fan: Tropospheric ozone trends at
718 Mauna Loa Observatory tied to decadal climate variability, *Nature Geosci.*, 7, 136-143,
719 doi:10.1038/NGEO2066, 2014.

720 Lin, M., A. M. Fiore, L. W. Horowitz, A. O. Langford, S. J. Oltmans, D. Tarasick, and H. E.
721 Reider: Climate variability modulates western US ozone air quality in spring via deep
722 stratospheric intrusions, *Nat. Commun.*, 67105, doi:10.1038/ncomms8105, 2015.

723 Liu, X., P. K. Bhartia, K. Chance, L. Froidevaux, R. J. D. Spurr, and T. P. Kurosu: Validation of
724 Ozone Monitoring Instrument (OMI) ozone profiles and stratospheric ozone columns with
725 Microwave Limb Sounder (MLS) measurements, *Atmos. Chem. Phys.*, 10, 2539-2549,
726 doi:10.5194/acp-10-2539-2010, 2010.

727 Liu, X., P. K. Bhartia, K. Chance, R. J. D. Spurr, and T. P. Kurosu: Ozone profile retrievals from
728 the Ozone Monitoring Instrument, *Atmos. Chem. Phys.*, 10, 2521-2537, doi:10.5194/acp-
729 10-2521-2010, 2010.

730 Logan, J. A., I. A. Megretskaja, A. J. Miller, G. C. Tiao, D. Choi, L. Zhang, R. S. Stolarski, G. J.
731 Labow, S. M. Hollandsworth, and G. E. Bodeker: Trends in the vertical distribution of
732 ozone: A comparison of two analyses of ozonesonde data, *J. Geophys. Res.*, 104, 26373-

733 263991999.

734 Mo, K. C., and R. E. Livezey: Tropical-extratropical geopotential height teleconnections during
735 the Northern Hemisphere winter, *Mon. Wea. Rev.*, 114, 2488-2515, doi:10.1175/1520-
736 0493(1986)114<2488:TEGHTD>2.0.CO;2, 1986.

737 [Nassar, R., J. A. Logan, I. A. Megretskaja, L. T. Murray, L. Zhang, and D. B. A. Jones: Analysis](#)
738 [of tropical tropospheric ozone, carbon monoxide, and water vapor during the 2006 El Niño](#)
739 [using TES observations and the GEOS-Chem model, *J. Geophys. Res.*, 114,](#)
740 [10.1029/2009JD011760, 2009.](#)

741 [Neu, J. L., T. Flury, G. L. Manney, M. L. Santee, N. J. Livesey, and J. Worden: Tropospheric](#)
742 [ozone variations governed by changes in stratospheric circulation, *Nature Geosci.*, 7, 340-](#)
743 [344, doi:10.1038/ngeo2138, 2014.](#)

744 Oman, L. D., J. R. Ziemke, A. R. Douglass, D. W. Waugh, C. Lang, J. M. Rodriguez, and J. E.
745 Nielsen: The response of tropical tropospheric ozone to ENSO, *Geophys. Res. Lett.*, 38,
746 10.1029/2011GL047865, 2011.

747 Oman, L. D., A. R. Douglass, J. R. Ziemke, J. M. Rodriguez, D. W. Waugh, and J. E. Nielsen:
748 The ozone response to ENSO in Aura satellite measurements and a chemistry-climate
749 simulation, *J. Geophys. Res. Atmos.*, 118, 965-976, doi:10.1029/2012JD018546, 2013.

750 Rienecker, M. M., M. J. Suarez, R. Gelaro, R. Todling, J. Bacmeister, E. Liu, M. G. Bosilovich,
751 S. D. Schubert, L. Takacs, G.-K. Kim, S. Bloom, J. Chen, D. Collins, A. Conaty, A. da
752 Silva, W. Gu, J. Joiner, R. D. Koster, R. Lucchesi, A. Molod, T. Owens, S. Pawson, P.
753 Pegion, C. R. Redder, R. Reichle, F. R. Robertson, A. G. Ruddick, M. Sienkiewicz, and J.
754 Woollen: MERRA: NASA's Modern-Era Retrospective Analysis for Research and
755 Applications, *J. Climate*, 24, 3624-3648, doi:10.1175/JCLI-D-11-00015.1, 2011.

756 Schoeberl, M. R., J. R. Ziemke, B. Bojkov, N. Livesey, B. Duncan, S. Strahan, L. Froidevaux, S.
757 Kulawik, P. K. Bhartia, S. Chandra, P. F. Levelt, J. C. Witte, A. M. Thompson, E. Cuevas,
758 A. Redondas, D. W. Tarasick, J. Davies, G. Bodeker, G. Hansen, B. J. Johnson, S. J.
759 Oltmans, H. Vömel, M. Allaart, H. Kelder, M. Newchurch, S. Godin-Beekmann, G.
760 Ancellet, H. Claude, S. B. Andersen, E. Kyrö, M. Parrondos, M. Yela, G. Zabolcki, D.
761 Moore, H. Dier, D. G. von, P., P. Viatte, R. Stübi, B. Calpini, P. Skrivankova, V. Dorokhov,

762 B. de, H., F. J. Schmidlin, G. Coetzee, M. Fujiwara, V. Thouret, F. Posny, G. Morris, J.
763 Merrill, C. P. Leong, G. Koenig-Langlo, and E. Joseph: A trajectory-based estimate of the
764 tropospheric ozone column using the residual method, *J. Geophys. Res.*, 112,
765 10.1029/2007JD008773, 2007.

766 Stajner, I., K. Wargan, S. Pawson, H. Hayashi, L.-P. Chang, R. C. Hudman, L. Froidevaux, N.
767 Livesey, P. F. Levelt, A. M. Thompson, D. W. Tarasick, R. Stübi, S. B. Andersen, M. Yela,
768 G. König-Langlo, F. J. Schmidlin, and J. C. Witte: Assimilated ozone from EOS-Aura:
769 Evaluation of the tropopause region and tropospheric columns, *J. Geophys. Res.*, 113,
770 10.1029/2007JD008863, 2008.

771 Stevenson, D., R. Doherty, M. Sanderson, C. Johnson, B. Collins, and D. Derwent: Impacts of
772 climate change and variability on tropospheric ozone and its precursors, *Faraday Discuss.*,
773 130, 41-57, doi:10.1039/B417412G, 2005.

774 Strahan, S. E., B. N. Duncan, and P. Hoor: Observationally derived transport diagnostics for the
775 lowermost stratosphere and their application to the GMI chemistry and transport model,
776 *Atmos. Chem. Phys.*, 7, 2435-2445, doi:10.5194/acp-7-2435-2007, 2007.

777 Strode, S. A., J. M. Rodriguez, J. A. Logan, O. R. Cooper, J. C. Witte, L. N. Lamsal, M. Damon,
778 B. Van Aartsen, S. D. Steenrod, and S. E. Strahan: Trends and variability in surface ozone
779 over the United States, *J. Geophys. Res. Atmos.*, 120, doi:10.1002/2014JD022784, 2015.

780 Sudo, K., and M. Takahashi: Simulation of tropospheric ozone changes during 1997–1998 El
781 Niño: Meteorological impact on tropospheric photochemistry, *Geophys. Res. Lett.*, 28,
782 4091-4094, doi:10.1029/2001GL013335, 2001.

783 Thompson, A. M., N. V. Balashov, J. C. Witte, J. G. R. Coetzee, V. Thouret, and F. Posny:
784 Tropospheric ozone increases over the southern Africa region: bellwether for rapid growth
785 in Southern Hemisphere pollution, *Atmos. Chem. Phys.*, 14, 9855-9869, 2014.

786 Thompson, A. M., J. C. Witte, R. D. Hudson, H. Guo, J. R. Herman, and M. Fujiwara: Tropical
787 Tropospheric Ozone and Biomass Burning, *Science*, 291, 2128-2132,
788 doi:10.1126/science.291.5511.2128, 2001.

789 Thompson, A. M., and R. D. Hudson: Tropical tropospheric ozone (TTO) maps from Nimbus 7

790 and Earth Probe TOMS by the modified-residual method: Evaluation with sondes, ENSO
791 signals, and trends from Atlantic regional time series, *J. Geophys. Res.*, 104, 26961-26975,
792 doi:10.1029/1999JD900470, 1999.

793 Tiao, G. C., G. C. Reinsel, D. Xu, J. H. Pedrick, X. Zhu, A. J. Miller, J. J. DeLuisi, C. L. Mateer,
794 and D. J. Wuebbles: Effects of autocorrelation and temporal sampling schemes on estimates
795 of trend and spatial correlation, *J. Geophys. Res.*, 95, 20507,
796 doi:10.1029/JD095iD12p20507, 1990.

797 Trenberth, K. E.: The Definition of El Niño, *Bull. Amer. Meteor. Soc.*, 78, 2771-2777,
798 doi:10.1175/1520-0477(1997)078<2771:TDOENO>2.0.CO;2, 1997.

799 Trenberth, K. E., G. W. Branstator, D. Karoly, A. Kumar, N.-C. Lau, and C. Ropelewski:
800 Progress during TOGA in understanding and modeling global teleconnections associated
801 with tropical sea surface temperatures, *J. Geophys. Res.*, 103, 14291-14324,
802 doi:10.1029/97JC01444, 1998.

803 Trenberth, K. E., J. M. Caron, D. P. Stepaniak, and S. Worley: Evolution of El Niño–Southern
804 Oscillation and global atmospheric surface temperatures, *J. Geophys. Res.*, 107,
805 10.1029/2000JD000298, 2002.

806 Vigouroux, C., T. Blumenstock, M. Coffey, Q. Errera, O. García, N. B. Jones, J. W. Hannigan, F.
807 Hase, B. Liley, E. Mahieu, J. Mellqvist, J. Notholt, M. Palm, G. Persson, M. Schneider, C.
808 Servais, D. Smale, L. Thölix, and M. De, M.: Trends of ozone total columns and vertical
809 distribution from FTIR observations at eight NDACC stations around the globe, *Atmos.*
810 *Chem. Phys.*, 15, 2915-2933, doi:10.5194/acp-15-2915-2015, 2015.

811 Wargan, K., S. Pawson, M. A. Olsen, J. C. Witte, A. R. Douglass, J. R. Ziemke, S. E. Strahan,
812 and J. E. Nielsen: The global structure of upper troposphere-lower stratosphere ozone in
813 GEOS-5: A multiyear assimilation of EOS Aura data, *J. Geophys. Res. Atmos.*, 120, 2013-
814 2036, doi:10.1002/2014JD022493, 2015.

815 Zeng, G., and J. A. Pyle: Influence of El Niño Southern Oscillation on stratosphere/troposphere
816 exchange and the global tropospheric ozone budget, *Geophys. Res. Lett.*, 32,
817 10.1029/2004GL021353, 2005.

818 Ziemke, J. R., S. Chandra, and P. K. Bhartia: Two new methods for deriving tropospheric column
819 ozone from TOMS measurements: Assimilated UARS MLS/HALOE and convective-cloud
820 differential techniques, *J. Geophys. Res.*, 103, 22115-22127, doi:10.1029/98JD01567, 1998.

821 Ziemke, J. R., S. Chandra, L. D. Oman, and P. K. Bhartia: A new ENSO index derived from
822 satellite measurements of column ozone, *Atmos. Chem. Phys.*, 10, 3711-3721,
823 doi:10.5194/acp-10-3711-2010, 2010.

824 Ziemke, J. R., A. R. Douglass, L. D. Oman, S. E. Strahan, and B. N. Duncan: Tropospheric ozone
825 variability in the tropics from ENSO to MJO and shorter timescales, *Atmos. Chem. Phys.*,
826 15, 8037-8049, doi:10.5194/acp-15-8037-2015, 2015.

827 Ziemke, J. R., M. A. Olsen, J. C. Witte, A. R. Douglass, S. E. Strahan, K. Wargan, X. Liu, M. R.
828 Schoeberl, K. Yang, T. B. Kaplan, S. Pawson, B. N. Duncan, P. A. Newman, P. K. Bhartia,
829 and M. K. Heney: Assessment and applications of NASA ozone data products derived from
830 Aura OMI/MLS satellite measurements in context of the GMI chemical transport model, *J.*
831 *Geophys. Res. Atmos.*, 119, 5671-5699, doi:10.1002/2013JD020914, 2014.

832 Ziemke, J. R., and S. Chandra: La Nina and El Nino induced variabilities of ozone in the tropical
833 lower atmosphere during 1970–2001, *Geophys. Res. Lett.*, 30, 1142,
834 doi:10.1029/2002GL016387, 2003.

835

836 **Figure captions**

837 **Fig. 1.** Time series of the Niño 3.4 index (K) from 1991 through 2013. The time period of ozone
838 analyses is the black line (2005-2013). The red line indicates the additional years covered by the
839 GMI simulation. Dashed lines are +0.75 and -0.75 that are considered strong El Niño and La
840 Niña conditions in this study.

841 **Fig. 2.** The 2005-2013 annual mean TCO (color contours) from the analyses. Black contours
842 indicate one standard deviation of the deseasonalized TCO expressed as a percent of the annual
843 mean TCO. Black contour interval is 0.5%.

844 **Fig. 3.** The deseasonalized TCO variance explained by ENSO from the linear regression over
845 2005-2013. Crosshatched areas denote where the confidence level of the explained variance
846 being different from zero is less than 95%. The increment of the white contours is 5%.

847 **Fig. 4.** The TCO sensitivity to the Niño 3.4 index from the linear regression over 2005-2013
848 (color contours). The sensitivity is expressed as the change in the TCO per degree change in the
849 index (DU K^{-1}). Crosshatched regions denote where the sensitivity is not statistically different
850 from zero at the 95% confidence level. White contours are incremented every 0.3 DU K^{-1} . The
851 streamlines show the difference between the mean winds at 200 hPa for months with strong El
852 Niño conditions (Niño 3.4 index greater than 0.75) minus months of strong La Niña conditions
853 (Niño 3.4 index less than -0.75). The thickness of the streamlines is scaled to the magnitude of
854 the difference. Particularly note the midlatitude regions of negative and positive sensitivity
855 aligned with anomalous cyclonic and anticyclonic circulations, as discussed in the text.

856 **Fig. 5.** Streamlines of the difference between the mean vertical and meridional winds for months
857 with strong El Niño conditions minus months of strong La Niña conditions from 2005-2013. The
858 means are calculated between 180° W and 120° W . The width of the streamlines is proportional
859 to the magnitude of the difference. The dashed line indicates the mean tropopause pressure for
860 strong El Niño months. Solid contours are the zonal mean wind for strong El Niño months.

861 **Fig. 6.** The dynamical (black) and convective (red) ozone tendency differences between months
862 of strong El Niño and La Niña conditions from the assimilation system over 2005-2013. The
863 means are calculated between 180° W and 120° W , matching that of Fig. 5.

864 **Fig. 7.** As in Fig. 5, but averaged between 85° E and 120° E .

865 **Fig. 8.** Difference in the outgoing longwave radiation (OLR) for months with strong El Niño
866 conditions minus months of strong La Niña conditions from 2005-2013. The differences are
867 expressed as percent of annual mean OLR. Thin white lines are incremented every 2%.

868 **Fig. 9.** The sensitivity of tropopause pressure to the Niño 3.4 index from linear regression over
869 2005-2013. The sensitivity is expressed as the change in tropopause pressure per degree change
870 in the index (hPa K^{-1}). Crosshatched regions denote where the sensitivity is not statistically
871 different from zero at the 95% confidence level. White contours are incremented every 2 hPa K^{-1} .
872

873 **Fig. 10.** The deseasonalized TCO variance explained by ENSO in the GMI CTM simulation for
874 years (a) 2005-2012 and (b) 1991-2012. Crosshatched areas denote where the confidence level of
875 the explained variance being different from zero is less than 95%. The increment of the white
876 contours is 5%.

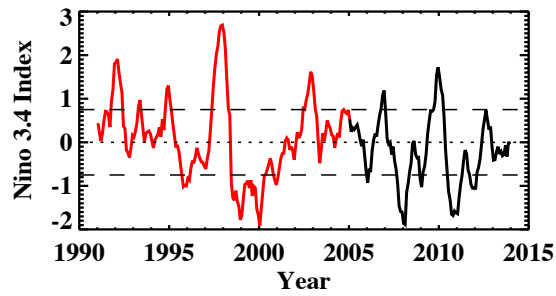


Figure 1. Time series of the Niño 3.4 index (K) from 1991 through 2013. The time period of ozone analyses is the black line (2005-2013). The red line spans the additional years covered by the GMI simulation. Dashed lines are +0.75 and -0.75 that are considered strong El Niño and La Niña conditions in this study.

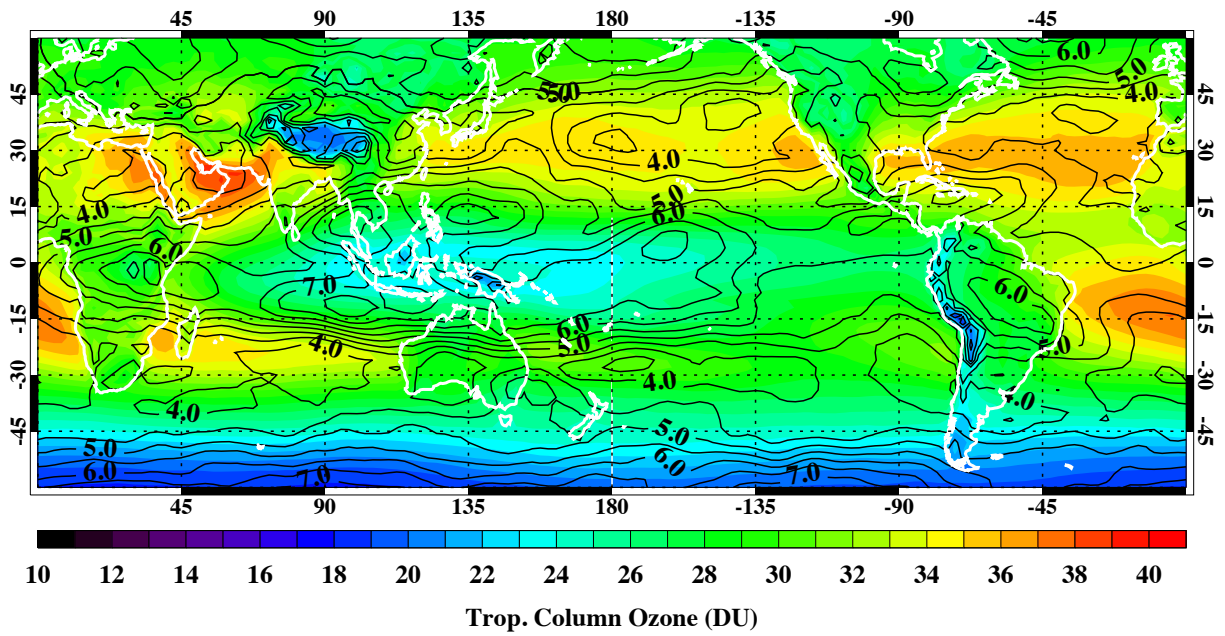


Figure 2. The 2005-2013 annual mean TCO (color contours) from the analyses. Black contours indicate one standard deviation of the deseasonalized TCO expressed as a percent of the annual mean TCO. Black contour interval is 0.5%.

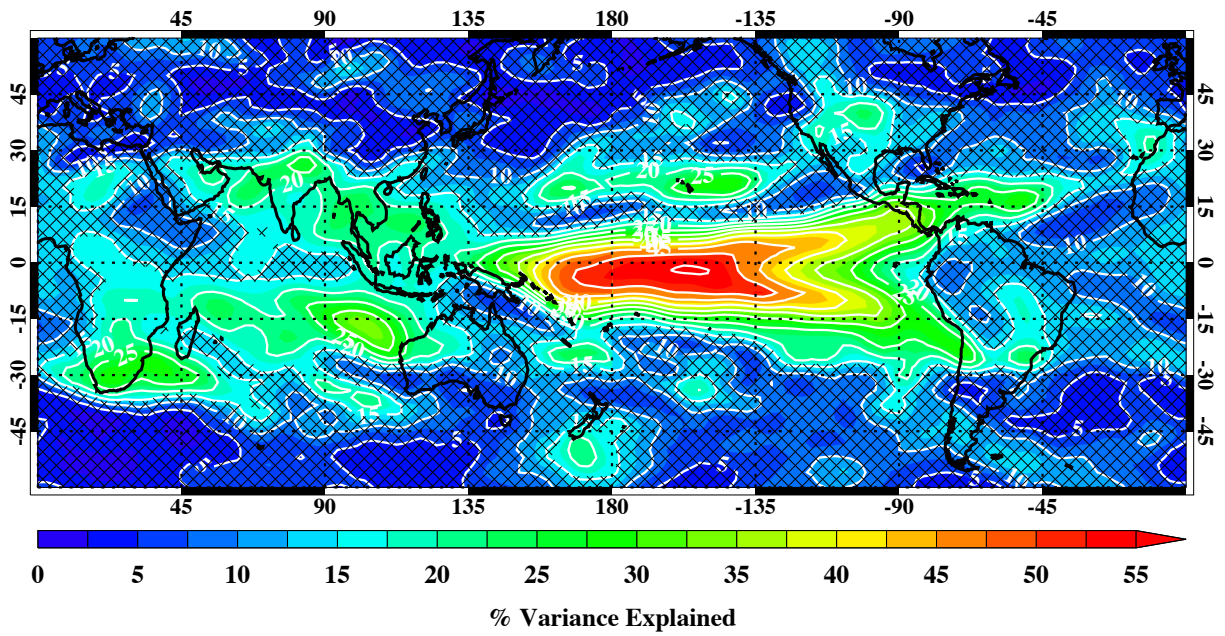


Figure 3. The deseasonalized TCO variance explained by ENSO from the linear regression over 2005-2013. Crosshatched areas denote where the confidence level of the explained variance being different from zero is less than 95%. The increment of the white contours is 5%.

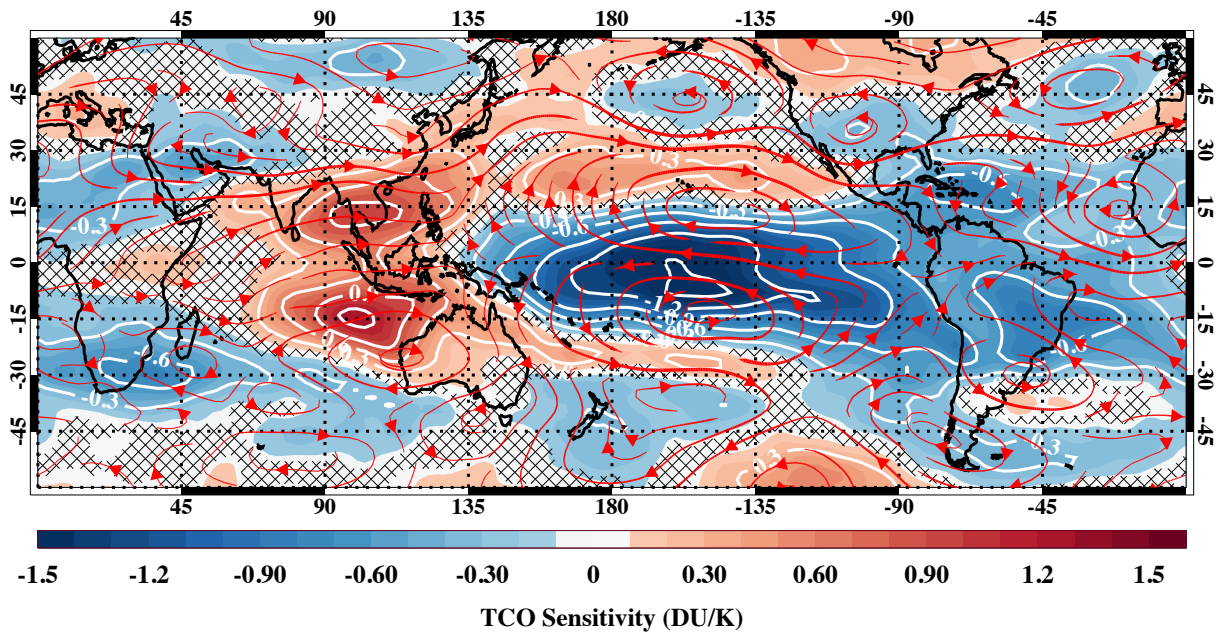


Figure 4. The TCO sensitivity to the Niño 3.4 index from the linear regression over 2005-2013 (color contours). The sensitivity is expressed as the change in the TCO per degree change in the index (DU/K). Crosshatched regions denote where the sensitivity is not statistically different from zero at the 95% confidence level. White contours are incremented every 0.3 DU/K. The streamlines show the difference between the mean winds at 200 hPa for months with strong El Niño conditions (Niño 3.4 index greater than 0.75) minus months of strong La Niña conditions (Niño 3.4 index less than -0.75). Particularly note the midlatitude regions of negative and positive sensitivity aligned with anomalous cyclonic and anticyclonic circulations, as discussed in the text.

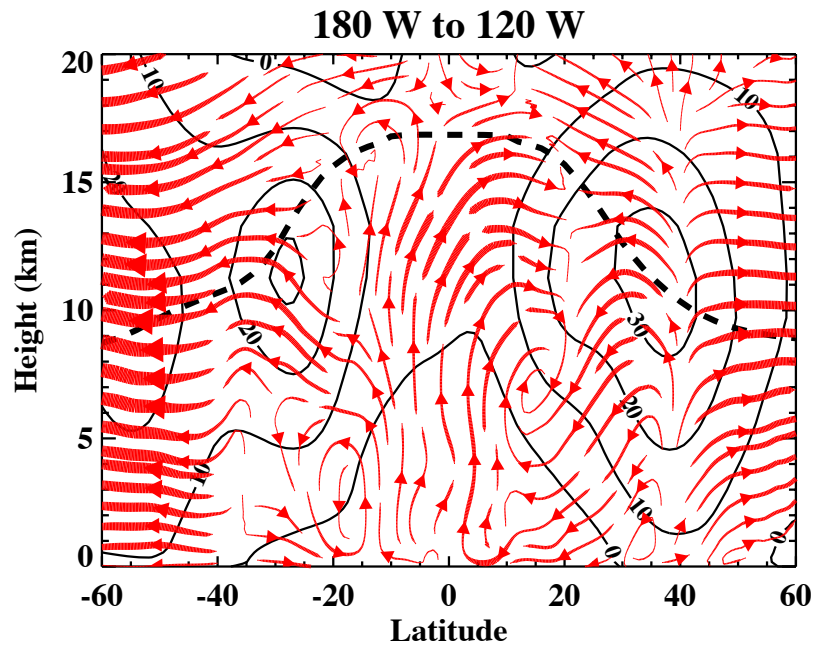


Figure 5. Streamlines of the difference between the mean vertical and meridional winds for months with strong El Niño conditions minus months of strong La Niña conditions from 2005-2013. The means are calculated between 180° W and 120° W. The width of the streamlines is proportional to the magnitude of the difference. The dashed line indicates the mean tropopause pressure for strong El Niño months. Solid contours are the zonal mean wind for extreme El Niño months.

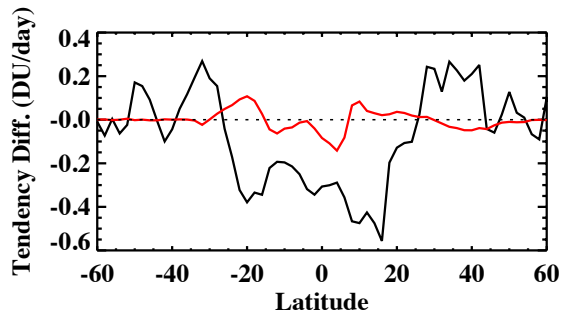


Figure 6. The dynamical (black) and convective (red) ozone tendency differences between months of strong El Niño and La Niña conditions from the assimilation system over 2005-2013. The means are calculated between 180° W and 120° W, matching that of Figure 4.

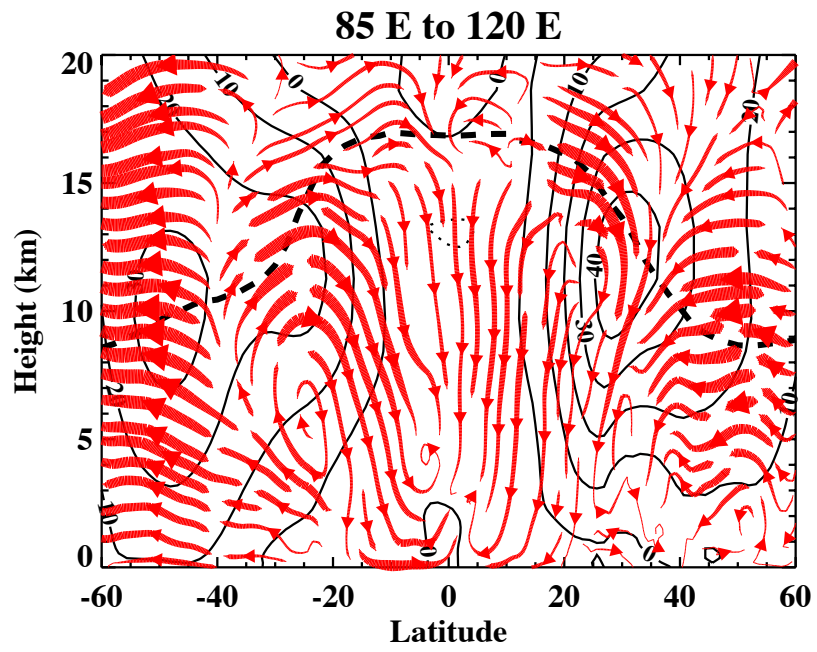


Figure 7. As in Figure 4, but averaged between 85° E and 120° E.

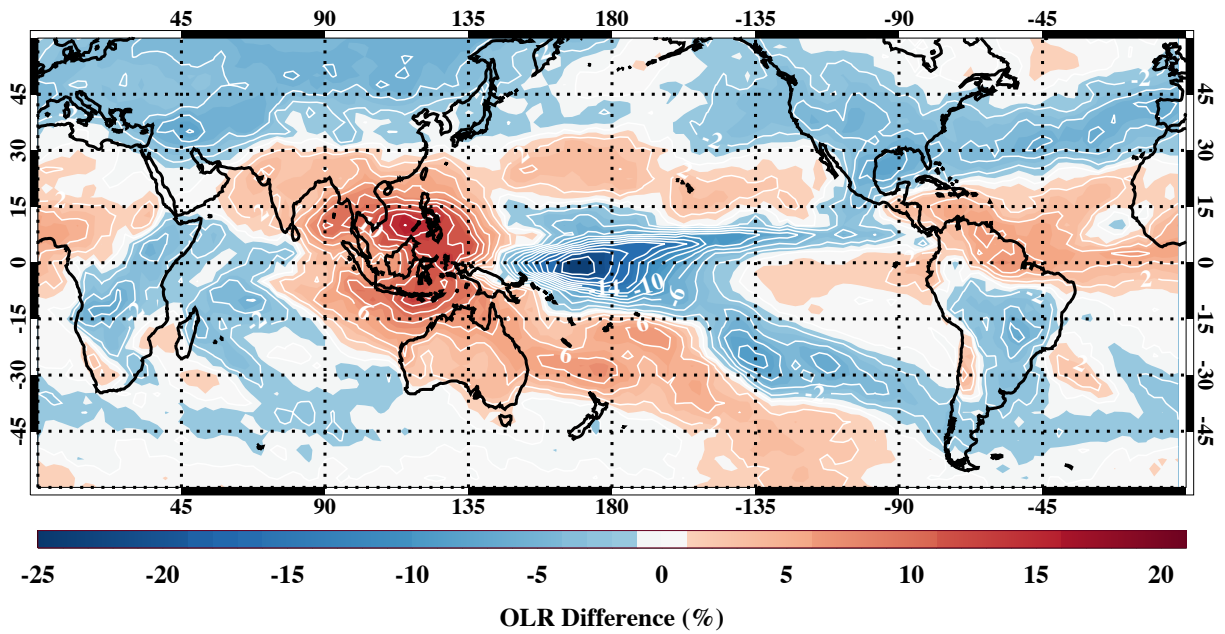


Figure 8. Difference in the outgoing longwave radiation (OLR) for months with strong El Niño conditions minus months of strong La Niña conditions from 2005-2013. The differences are expressed as percent of annual mean OLR. Thin white lines are incremented every 2%.

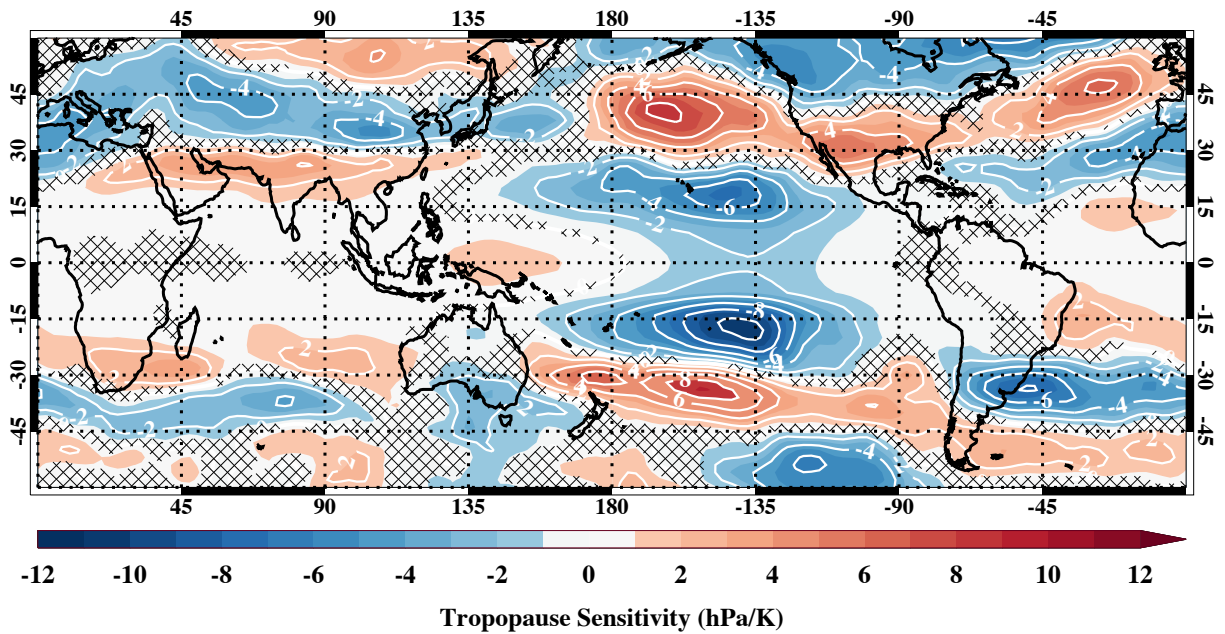


Figure 9. The sensitivity of tropopause pressure to the Niño 3.4 index from linear regression over 2005-2013. The sensitivity is expressed as the change in tropopause pressure per degree change in the index (hPa/K). Crosshatched regions denote where the sensitivity is not statistically different from zero at the 95% confidence level. White contours are incremented every 2 hPa/K.

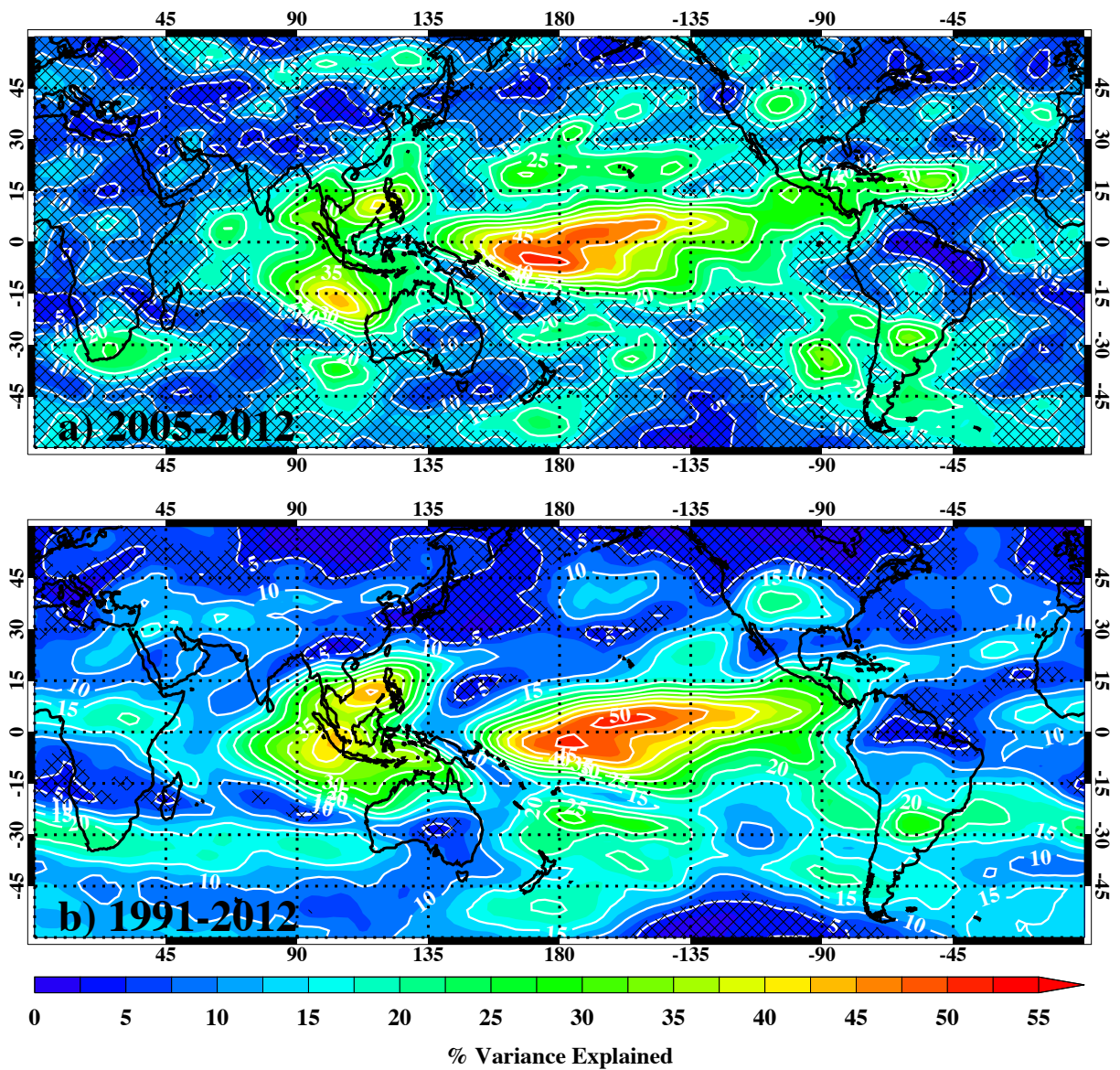


Figure 10. The deseasonalized TCO variance explained by ENSO in the GMI CTM simulation for years (a) 2005-2012 and (b) 1991-2012. Crosshatched areas denote where the confidence level of the explained variance being different from zero is less than 95%. The increment of the white contours is 5%.